Differential coding of absolute and relative aversive value in the Drosophila brain

Maria Villar, Miguel Pavão-Delgado, Marie Amigo, Pedro Jacob, Nesrine Merabet, Anthony Pinot, Sophie Perry, Scott Waddell, Emmanuel Perisse

Article

Current Biology

Differential coding of absolute and relative aversive value in the *Drosophila* brain

Graphical abstract

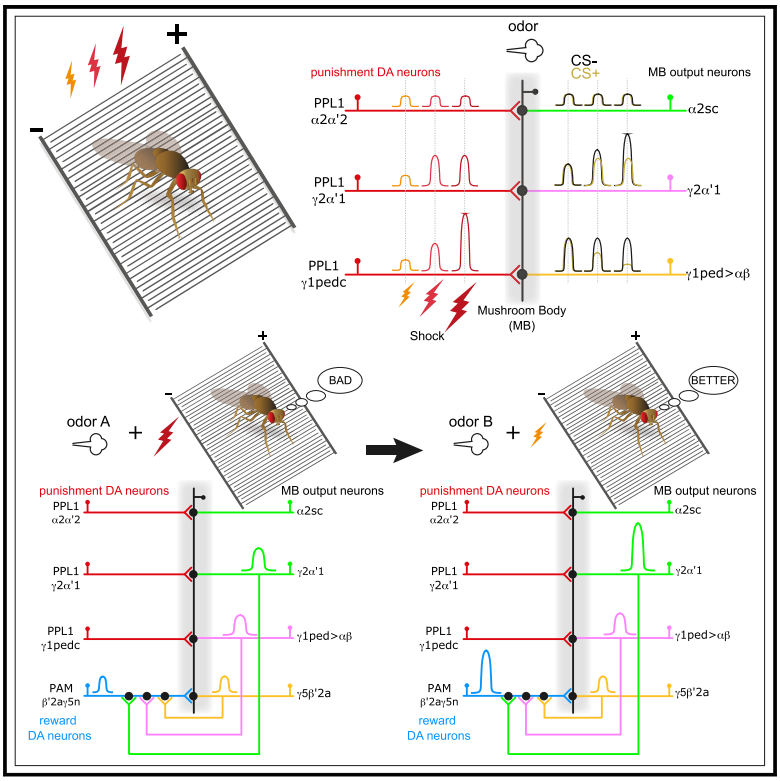

Highlights

- Individual dopaminergic neurons respond differently to punishment intensity
- Learning-induced plasticity is scaled to punishment intensity
- Specific dopaminergic neurons signal “better than” aversive value
- Opposing network interactions enable relative value coding

Authors

Maria E. Villar, Miguel Pavão-Delgado, Marie Amigo, ..., Sophie A. Perry, Scott Waddell, Emmanuel Perisse

Correspondence

emmanuel.perisse@igf.cnrs.fr

In brief

Optimal decision making requires animals to learn and use memories of absolute (good or bad) and relative (better or worse) experience. Villar et al. show that interaction between groups of valence-specific *Drosophila* dopaminergic neurons encodes absolute and relative aversive value teaching signals during learning.

Villar et al., 2022, Current Biology *32*, 1–17
November 7, 2022
https://doi.org/10.1016/j.cub.2022.08.058

CellPress

Please cite this article in press as: Villar et al., Differential coding of absolute and relative aversive value in the *Drosophila* brain, Current Biology (2022), https://doi.org/10.1016/j.cub.2022.08.058

Current Biology

CellPress
OPEN ACCESS

Article

Differential coding of absolute and relative aversive value in the *Drosophila* brain

Maria E. Villar,[1,4] Miguel Pavão-Delgado,[1,4,5] Marie Amigo,[1] Pedro F. Jacob,[2] Nesrine Merabet,[1] Anthony Pinot,[1,3] Sophie A. Perry,[2] Scott Waddell,[2] and Emmanuel Perisse[1,2,6,7,*]

[1]Institute of Functional Genomics, University of Montpellier, CNRS, INSERM, 141 rue de la Cardonille, 34094 Montpellier Cedex 5, France
[2]Centre for Neural Circuits & Behavior, University of Oxford, Oxford OX1 3TA, UK
[3]BioCampus Montpellier, University of Montpellier, CNRS, INSERM, 34094 Montpellier, France
[4]These authors contributed equally
[5]Present address: Friedrich Miescher Institute for Biomedical Research, Basel, Switzerland and Faculty of Science, University of Basel, Basel, Switzerland
[6]Twitter: @ManuPerisse
[7]Lead contact
*Correspondence: emmanuel.perisse@igf.cnrs.fr
https://doi.org/10.1016/j.cub.2022.08.058

SUMMARY

Animals use prior experience to assign absolute (good or bad) and relative (better or worse) value to new experience. These learned values guide appropriate later decision making. Even though our understanding of how the valuation system computes absolute value is relatively advanced, the mechanistic underpinnings of relative valuation are unclear. Here, we uncover mechanisms of absolute and relative aversive valuation in *Drosophila*. Three types of punishment-sensitive dopaminergic neurons (DANs) respond differently to electric shock intensity. During learning, these punishment-sensitive DANs drive intensity-scaled plasticity at their respective mushroom body output neuron (MBON) connections to code absolute aversive value. In contrast, by comparing the absolute value of current and previous aversive experiences, the MBON-DAN network can code relative aversive value by using specific punishment-sensitive DANs and recruiting a specific subtype of reward-coding DANs. Behavioral and physiological experiments revealed that a specific subtype of reward-coding DAN assigns a "better than" value to the lesser of the two aversive experiences. This study therefore highlights how appetitive-aversive system interactions within the MB network can code and compare sequential aversive experiences to learn relative aversive value.

INTRODUCTION

Value-based decisions require animals to make choices between several options based on a prediction of their relative subjective value learned through prior experience.[1] Associative learning provides a means to assign absolute (good or bad) values to experience that can be used to guide future approach or avoidance behaviors.[2] During learning, animals can also compare the value of their current experience with that of prior knowledge and assign a relative value (better or worse) between these experiences to promote more accurate economic-based choices.[3–9] Notwithstanding that a substantial body of research has investigated mechanisms for relative reward-value coding,[3,10–19] we know less about how relative aversive value is computed during learning to guide appropriate value-based decisions.[5,20–23] Reinforcement learning models propose that learning occurs when actual outcome value differs from predicted value.[24,25] This process and the error computed between actual and predicted value are driven by a valuation circuit that includes dopaminergic and GABAergic neurons.[26–28] However, it is unclear whether similar circuitry compares current and previous experience to assign relative aversive value to sensory stimuli during learning.

Anatomically discrete dopaminergic neurons (DANs) in *Drosophila* and mice provide either positive or negative teaching signals (for reviews, see Waddell,[29] Watabe-Uchida and Uchida,[30] Brooks and Berns,[31] and Adel and Griffith[32]). In flies, these different DANs project to unique compartments of the mushroom body (MB), a central brain structure essential for olfactory learning and memory as well as several goal-directed behaviors.[33–35] DANs from the protocerebral posterior lateral 1 (PPL1) cluster projecting to the vertical and proximal horizontal lobes of the MB relay punishment and signal negative value during learning.[36–41] Many DANs from the protocerebral anterior medial (PAM) cluster projecting to the horizontal lobes of the MB assign positive reward value during learning.[42–49] Sparse activation within the ~4,000 MB intrinsic Kenyon cells (KCs), which indirectly receive odorant information from sensory neurons in the periphery, provides the specificity of olfactory memories.[21,50,51] KCs synapse onto mushroom body output neurons (MBONs), which project into downstream structures[52] to drive (for most of them) approach or avoidance behavior,[35,47,53] but see Hattori et al.[54] Some MBONs are synaptically interconnected, providing cross-excitation or -inhibition between MB compartments.[47,53,55] Lastly, many MBONs make feedback or feedforward synapses outside the MB onto DAN

Please cite this article in press as: Villar et al., Differential coding of absolute and relative aversive value in the *Drosophila* brain, Current Biology (2022), https://doi.org/10.1016/j.cub.2022.08.058

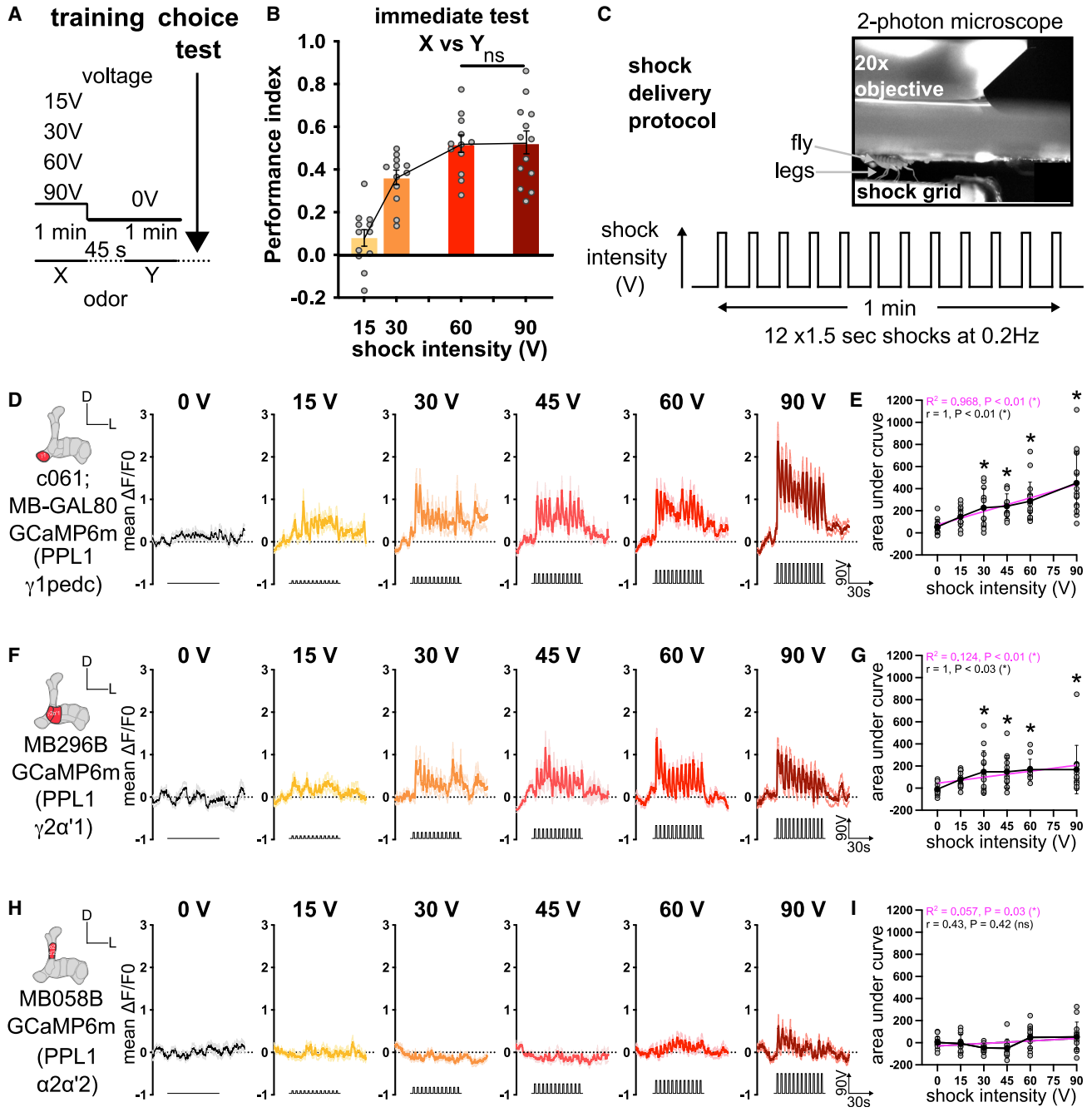

Figure 1. PPL1-γ1pedc, PPL1-γ2α′1, and PPL1-α2α′2 DANs respond differently to electric shock intensity

(A) Training procedure of differential conditioning; odor X is paired with either 15, 30, 60, or 90 V. Odor Y is presented alone.

(B) Memory performance immediately after training. Flies choose between odors X and Y in a T-maze. Performance increases with shock intensity reaching a plateau at 60 V. n = 12 (15 V), 12 (30 V), 12 (60 V), and 13 (90 V).

(C) Experimental setup for *in vivo* calcium imaging. Flies are presented with electric shocks to the legs, while neural activity is recorded in DANs expressing GCaMP6m.

(D) Mean ΔF/F0 calcium transients ± standard error of the mean (SEM) measured from PPL1-γ1pedc targeted by c061;MBGAL80-GAL4 as flies were exposed to 0, 15, 30, 45, 60, and 90 V shocks.

(E) Mean area under the curve ± standard deviation (SD) during the 1 min of 12 shocks for PPL1-γ1pedc DANs (n = 13, 15, 12, 13, 17, and 15). PPL1-γ1pedc DAN responses show a strong and significant correlation with shock intensity (Spearman correlation). Kruskal-Wallis test and Dunn's multiple comparisons test against 0 V.

(F) Mean ΔF/F0 calcium transients ± SEM measured from PPL1-γ2α′1 targeted by MB296B-GAL4 as flies were exposed to 0, 15, 30, 45, 60, and 90 V shocks.

(G) Mean area under the curve ± SD during the 1 min of 12 shocks for PPL1-γ2α′1 (n = 13 for all groups). PPL1-γ2α′1 DAN responses showing a strong and significant correlation with shock intensity (Spearman correlation). Kruskal-Wallis test and Dunn's multiple comparisons test against 0 V.

(legend continued on next page)

Please cite this article in press as: Villar et al., Differential coding of absolute and relative aversive value in the *Drosophila* brain, Current Biology (2022), https://doi.org/10.1016/j.cub.2022.08.058

dendrites.[47,49,55–59] During olfactory associative learning, specific DANs releasing dopamine in individual MB compartments depress synaptic strengths between sparse odor-activated KCs and the MBONs whose dendrites reside within the relevant compartments.[53,59–67] As a result, learning-induced plasticity within different MB compartments reconfigures the MBON ensemble output signal to promote either learned approach or avoidance behavior.[35,68] Olfactory aversive learning reduces odor drive of approach-directing MBONs,[53,62] hence tilting the MBON network toward promoting odor avoidance. By contrast, appetitive learning reduces odor drive of avoidance-directing MBONs, leaving the network in a configuration promoting odor approach.

Flies can perceive, learn, and compare differences in the intensity of punishment and adapt their behavior accordingly.[8,21,69–72] Here, we combined genetic interventions with behavioral analyses, anatomical characterization, and *in vivo* two-photon calcium imaging to investigate the detailed circuit requirements that allow flies to write and compare olfactory aversive memories of different intensities during learning to promote appropriate value-based choices. We found that aversive PPL1 DANs show differential responses to electric shock punishment of varying intensity. As a result, the intensity of shock reinforcement correlates with the magnitude of learning-driven plasticity at the corresponding KC to MBON junctions. Using a specific behavioral paradigm in which flies associate three odors with 0, 60, and 30 V punishment, respectively, we identified the circuits involved in coding relative aversive value. Loss-of-function screening revealed a role for specific aversive DANs, in addition to the rewarding PAM-β′2aγ5n DANs, to learn relative aversive value. Recording from PAM-β′2aγ5n DANs during learning revealed these neurons to signal relative aversive value by increasing their responsiveness when the odor-low shock association is better than a previous odor-high shock association. Recording from three MBONs presynaptic to PAM-β′2aγ5n DANs revealed a positive difference in the odor responses of MBON-γ2α′1 between current and previous aversive experiences. This increased responsiveness of cholinergic MBON-γ2α′1 likely provides excitatory input necessary to drive the PAM-β′2aγ5n DANs "better than" value signal for the less aversive experience, and they thereby learn relative aversive value. In support of this model, optogenetic activation of PAM-β′2aγ5n reward DANs, during learning, assigns a relative "better than" value to one of two identical odor-punishment associations.

RESULTS

Individual PPL1 DANs respond differently to electric shock intensity

Flies can learn to associate odors with different intensities of electric shocks, reaching a plateau of memory performance around 60 V (Figures 1A and 1B).[8,69,70,73] Some PPL1 DANs respond to different current intensity.[74,75] However, it is currently unknown how shock-responsive DANs in the PPL1 cluster assign aversive values of different intensities to odors during learning. To monitor DAN responses in a setting resembling standard training conditions[69] (i.e., with different voltage intensities), we used two-photon microscopy and expressed GCaMP6m[76] in punishment-sensitive DANs. We measured calcium responses following electric shocks of 0, 15, 30, 45, 60, or 90 V delivered to the fly legs (Figure 1C). Imaging focused on three DANs from the PPL1 cluster, two of which—PPL1-γ1pedc and PPL1-γ2α′1— are known to assign negative value to odors during learning,[37,39] whereas the third—PPL1-α2α′2—does not exhibit clear immediate reinforcing properties when artificially triggered alone.[40,62] In these experiments, each fly is only presented with one voltage (intensity) and therefore each shock experience is equivalent. We found that calcium transients in both PPL1-γ1pedc and PPL1-γ2α′1, but not in PPL1-α2α′2 DANs, significantly increased with electric shock stimulation above 30 V, fitting with a linear regression (magenta) and correlating with shock intensity (r value in black) (Figures 1D–1I). Although not reaching significance, PPL1-α2α′2 DAN responses seem to be synchronized with shock stimulations of 60 and 90 V, hence a fitted regression line (magenta) with a slope different from 0 but a very low R^2. For all DANs, the increased response was observable from the first of the twelve shock presentations for each intensity (Figures S1A–S1F). While proportional shock responses were readily apparent in PPL1-γ1pedc DANs (Figures 1D and 1E), PPL1-γ2α′1 DAN responses remained stable from 30 to 90 V (Figures 1F and 1G). Accordingly, comparing the slopes of the corresponding fitted regression lines for each DAN response (in magenta in Figures 1E, 1G, and 1I), revealed a significant difference between PPL1-γ1pedc and PPL1-γ2α′1, and between PPL1-γ1pedc and PPL1-α2α′2 DAN responses, whereas PPL1-γ2α′1 and PPL1-α2α′2 DANs were indistinguishable (Figure S1G). We noted that PPL1-γ1pedc and PPL1-γ2α′1 DANs respond similarly during the first shock (Figure S1H). Overall, these data show that PPL1-γ1pedc, PPL1-γ2α′1, and PPL1-α2α′2 DANs respond differently to a range of electric shock intensities and demonstrate a functional segregation between these three types of PPL1 DANs.

Learning-induced plasticity at the KC to MBON-γ1ped>αβ and MBON-γ2α′1 junctions scales with shock intensity

During olfactory associative learning, dopamine from punishment or reward DANs drives synaptic depression between sparse odor-activated KCs and the corresponding MBONs in the relevant compartments to promote appropriate learned behavior.[47,49,53,60,62–65,67] We therefore tested whether PPL1-γ1pedc, PPL1-γ2α′1, and PPL1-α2α′2 DANs might induce intensity-dependent plasticity of MBON-γ1ped>αβ, MBON-γ2α′1, and MBON-α2sc (Figures S2A–S2C) odor responses following training with different voltages. Flies were trained under a two-photon microscope[47] (Figure 2A) using a differential conditioning

(H) Mean ΔF/F0 calcium transients ± SEM measured from PPL1-α2α′2 targeted by MB058B-GAL4 as flies were exposed to 0, 15, 30, 45, 60, and 90 V shocks.
(I) Mean area under the curve ± SD during the 1 min of 12 shocks for PPL1-α2α′2 (n = 14, 12, 13, 10, 14, and 13). PPL1-α2α′2 DAN responses show no correlation with the shock intensity (Spearman correlation). Kruskal-Wallis test and Dunn's multiple comparisons test against 0 V.
Linear regression slopes (magenta) are tested against 0. Individual data points are displayed as dots. * $p < 0.05$. ns: non-significant.
See also Figure S1 and Table S1.

Please cite this article in press as: Villar et al., Differential coding of absolute and relative aversive value in the *Drosophila* brain, Current Biology (2022), https://doi.org/10.1016/j.cub.2022.08.058

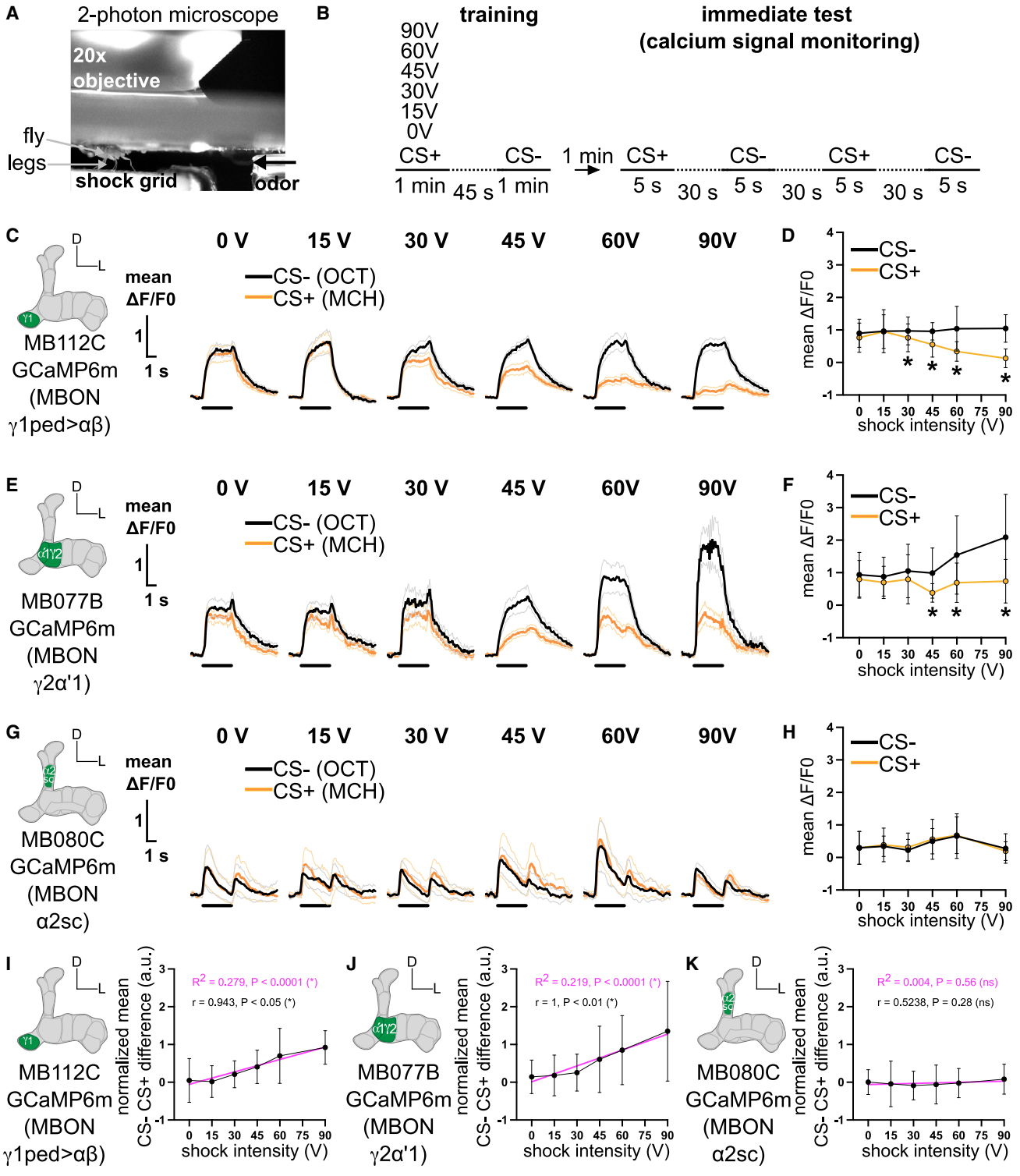

Figure 2. Aversive learning drives intensity-dependent plasticity of MBON-γ1ped>αβ and MBON-γ2α′1 odor responses

(A) Experimental setup. Odor and electric shock punishment are paired under the two-photon microscope.

(B) Protocol: flies are trained to associate a 1 min odor presentation (CS+, here MCH) paired with electric shocks of 0, 15, 30, 45, 60, or 90 V delivered to the legs, followed by a 45 s presentation of fresh air and then another odor without shocks (CS−, here OCT). Immediately (1 min) after training, neural activity is recorded in MBONs expressing GCaMP6m during 5 s presentations of the CS+ and CS−, performed twice and spaced by 30 s.

(C) Mean ΔF/F0 calcium transients ± SEM for the CS− (average of the two presentations, black) and for the CS+ (average of the two presentations, orange) immediately after training the CS+ with either 0, 15, 30, 45, 60, or 90 V for MBON-γ1ped>αβ targeted by MB112C-GAL4.

(legend continued on next page)

Please cite this article in press as: Villar et al., Differential coding of absolute and relative aversive value in the *Drosophila* brain, Current Biology (2022), https://doi.org/10.1016/j.cub.2022.08.058

paradigm where only the first of two odors was paired with a differing intensity of shock, the Condition Stimulus + (CS+) (Figure 2B). We then immediately performed *in vivo* calcium imaging to measure odor-evoked responses in these three MBONs. In line with previous work,[47,53] we observed robust depression of the CS+ relative to the CS− (unpaired odor) responses in MBON-γ1ped>αβ when flies were trained with a 30 V or higher shock (Figures 2C and 2D). Moreover, there was a strong correlation (r = 0.94) between the CS− CS+ response difference and the intensity of shock reinforcement (Figure 2I). These results were recapitulated with the reciprocal pairing of odors as the CS+ and CS− (Figures S2D, S2E, and S2H). MBON-γ2α′1 exhibited a significant difference in odor-evoked responses between CS+ and CS− when training was performed with 45 V and higher voltages (Figures 2E and 2F), again a result largely recapitulated in experiments with the opposite odors employed as CS+ and CS− (Figures S2F, S2G, and S2I). A smaller difference was evident: there was a greater CS− increase after training when methylcyclohexanol (MCH) was the CS+ (Figures 2E and 2F) compared with when 3-octanol (OCT) was the CS+ (Figures S2F and S2G). Nevertheless, both odor sequences showed a high and significant correlation (r = 1 and r = 0.99) between the CS− CS+ response difference and the intensity of shock (Figures 2J and S2I). These results, combined with our behavioral observations and PPL1 DAN recordings (Figures 1B and 1D–1G), suggest that threshold activation of PPL1-γ1pedc (30 V) and PPL1-γ2α′1 (45 V) during learning is necessary to induce a behaviorally relevant memory trace in the KC to MBON-γ1ped>αβ and MBON-γ2α′1 connections. Similar experiments did not reveal learning-induced plasticity in MBON-α2sc odor responses (Figures 2G, 2H, and 2K), in agreement with the relative absence of PPL1-α2α′2 DAN shock responses irrespective of shock intensity (Figures 1H and 1I).

Building a correlation matrix for all PPL1 DAN responses and all MBON CS− CS+ response differences, we found a high and significant correlation between the DAN responses and MBON changes in the γ1pedc and γ2α′1, but not α2α′2, compartments (Figures S2J and S2K). Overall, these data lead us to conclude that aversive memories of different electric shock intensity are written in a graded manner at the KC to MBON-γ1ped>αβ and MBON-γ2α′1 junctions by the respective DANs whose activation scales with the intensity of electric shock. The combined intensity-dependent plasticity of odor-evoked responses in these MBONs will proportionally skew the overall MBON output to promote appropriate choices between the CS+ and CS− odors in the T-maze.

Punishing and rewarding DANs are required to learn relative aversive value

Intensity-dependent differential synaptic plasticity at multiple MB compartments could provide a substrate to compare and compute a relative aversive value between olfactory experiences during learning, which can later be used during decision-making in the T-maze. To test this possibility and probe the underlying neural mechanisms, we used a relative aversive learning task. Flies were trained to associate three different odors (X, Y, and Z) with different intensities of electric shock (0, 60, and 30 V, respectively) (Figures S3A and S3B).[8,21] In a T-maze, the flies were then given either a relative choice between the Y_{60} versus Z_{30} odors or an absolute choice between the X_0 versus Y_{60} odors. (Note: although there is a "relative" choice between the non-reinforced odor X and odor Y previously punished with 60 V, we give this choice the "absolute" label to distinguish it from the relative choice between two previously punished odors Y_{60} versus Z_{30}.) We first assessed the requirement of all PPL1 (Figure 3A) or PAM (Figure 3B) DANs during learning. Output of DANs was temporally blocked 30 min prior to and during training, using expression of the dominant temperature-sensitive UAS-*Shibire*^{ts1} (*Shi*^{ts1})[77] at the restrictive temperature of 33°C. Flies were returned to permissive 23°C immediately after training and 30 min later were given a T -maze odor choice (Figure 3C). As expected, blocking all aversive PPL1DANs (MB504B-GAL4) during training impaired performance in both relative and absolute choice tests, compared with that of controls carrying only the GAL4 or *Shi*^{ts1} transgene (Figures 3D and 3E). However, blocking PAM DANs (R58E02-GAL4) during training left absolute choices intact but abolished performance in the relative choice test (Figures 3D and 3E).[21] Importantly, control experiments performed at permissive 23°C did not reveal significant differences between the groups (Figures S3C–S3E). Therefore, both reward and punishment coding DANs are necessary during learning to support appropriate relative choice.

PPL1-γ1pedc, PPL1-γ2α′1, and PPL1-α2α′2 aversive DANs are required to learn relative aversive value

Prior work has defined the DANs conveying aversive reinforcement as the 4 different subtypes from the PPL1 cluster and a few neurons from the PAM cluster (Figure 4A).[39] We used *Shi*^{ts1} to block output PPL1-γ1pedc (Figure S4A), PPL1-γ2α′1

(D) Mean ΔF/F0 ± SD during the 5 s odor presentation for the CS− (black) and for the CS+ (orange) when paired with either 0, 15, 30, 45, 60, and 90 V for MBON-γ1ped>αβ (n = 17, 14, 15, 16, 18, and 14). Unpaired t test (or Wilcoxon test) between the CS− and the CS+ for each voltage intensity.
(E) Mean ΔF/F0 calcium transients ± SEM for the CS− (average of the two presentations, black) and for the CS+ (average of the two presentations, orange) immediately after training the CS+ with either 0, 15, 30, 45, 60, or 90 V for MBON-γ2α′1 targeted by MB077B-GAL4.
(F) Mean ΔF/F0 ± SD during the 5 s odor presentation for the CS− (black) and for the CS+ (orange) when paired with either 0, 15, 30, 45, 60, and 90 V for MBON-γ2α′1 (n = 19, 16, 14, 15, 17, and 16). Unpaired t test (or Wilcoxon test) between the CS− and the CS+ for each voltage intensity.
(G) Mean ΔF/F0 calcium transients ± SEM for the CS− (average of the two presentations, black) and for the CS+ (average of the two presentations, orange) immediately after training the CS+ with either 0, 15, 30, 45, 60, or 90 V for MBON-α2sc targeted by MB080C-GAL4.
(H) Mean ΔF/F0 ± SD during the 5 s odor presentation for the CS− (black) and for the CS+ (orange) when paired with either 0, 15, 30, 45, 60, and 90 V for MBON-α2sc (n = 12, 11, 13, 11, 12, and 12). Unpaired t test (or Wilcoxon test) between the CS− and the CS+ for each voltage intensity.
(I–K) Normalized CS− CS+ difference ± SD and fitted linear regression for MBON-γ1ped> αβ, MBON-γ2α′1, and MBON-α2sc with a Pearson (r) (or Spearman) correlation. Linear regression slopes (magenta) are tested against 0.
*p < 0.05. ns: non-significant.
See also Figure S2 and Table S1.

Please cite this article in press as: Villar et al., Differential coding of absolute and relative aversive value in the *Drosophila* brain, Current Biology (2022), https://doi.org/10.1016/j.cub.2022.08.058

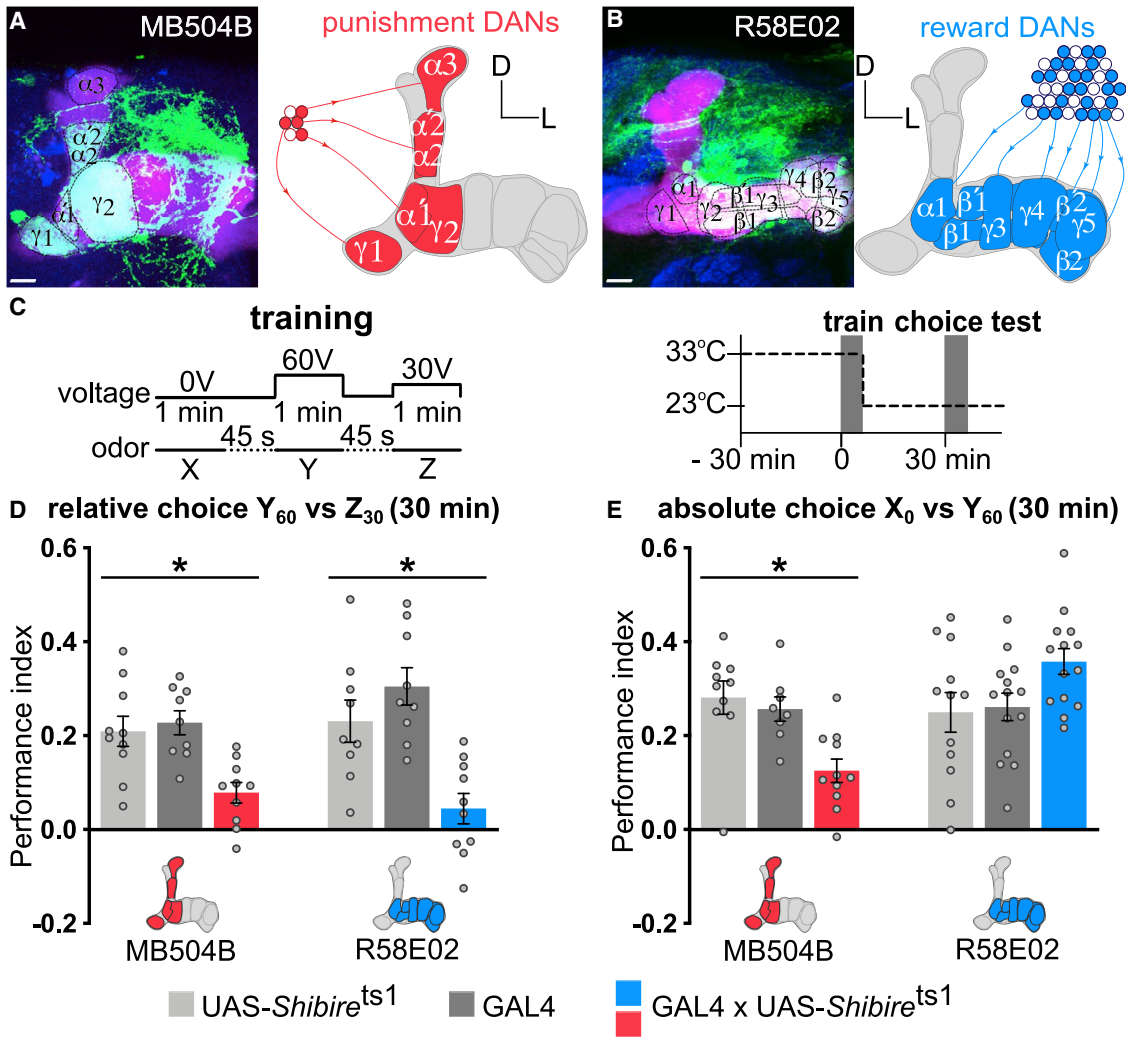

Figure 3. Aversive and reward DANs are required to learn relative aversive value, whereas absolute value learning requires only aversive DANs

(A and B) MB504-GAL4 driving UAS-mCD8::GFP labeling all PPL1 punishment DANs (schematized in red with the MB in gray) and R58E02-GAL4 driving UAS-mCD8::GFP labeling most reward PAM DANs (schematized in blue with the MB in gray). The right MB is co-labeled with 247-LexA::VP16-driven lexAop-rCD2::mRFP (magenta) and the whole brain with the presynaptic marker anti-Bruchpilot, nc82 (blue). Scale bars, 10 μm.

(C) Training protocol and temperature shifting procedure for *Shi*^{ts1} manipulations.

(D) Blocking output from MB504B- or R58E02-GAL4 DANs during training impaired 30 min relative choice, compared with that of relevant controls (both one-way ANOVA, n = 9–10, $p < 0.05$). Data are mean ± SEM. Individual data points are displayed as dots. * $p < 0.05$.

(E) Blocking output from MB504B- but not R58E02-GAL4 during training impaired 30 min absolute choice, compared with that of relevant controls (Kruskal-Wallis, n = 8–11, $p < 0.05$ and one-way ANOVA, n = 12–14, $p > 0.05$, respectively). Data are mean ± SEM. Individual data points are displayed as dots. * $p < 0.05$. See also Figure S3 and Table S1.

(Figure S4B), PPL1-α2α′2 (Figure S4C), PPL1-α3 (Figure S4D), and PAM-β2β′2a (Figures S4E and S4F) DANs (we did not test PAM-γ3[48]) during learning and assessed the consequence in a relative or absolute odor choice test 30 min after training (Figure 4B). Blocking PPL1-γ1pedc DANs during learning reduced both relative and absolute choices (Figures 4C and 4D). By contrast, blocking PPL1-γ2α′1 or PPL1-α2α′2, but not PPL1-α3 or PAM-β2β′2a, during learning left absolute choices unchanged but abolished relative choices (Figures 4C, 4D, and S4G–S4I). No performance defects were apparent when the entire experiment was performed at permissive 23°C (Figures S4J–S4L). Together, these results reveal PPL1-γ1pedc as critical for signaling absolute and relative aversive value, whereas PPL1-γ2α′1 and PPL1-α2α′2 are only required to learn relative aversive value.

PAM-β′2aγ5n rewarding DANs are required to learn relative value

We next tested which specific rewarding PAM DANs (Figure 5A) were required to learn relative aversive value. We again used *Shi*^{ts1} to block output of discrete subpopulations of DANs (0104-GAL4, R56H09-GAL4, and 0279-GAL4[21,43,44,78] (Figures S5A, S5B, and

Please cite this article in press as: Villar et al., Differential coding of absolute and relative aversive value in the *Drosophila* brain, Current Biology (2022), https://doi.org/10.1016/j.cub.2022.08.058

CellPress
OPEN ACCESS

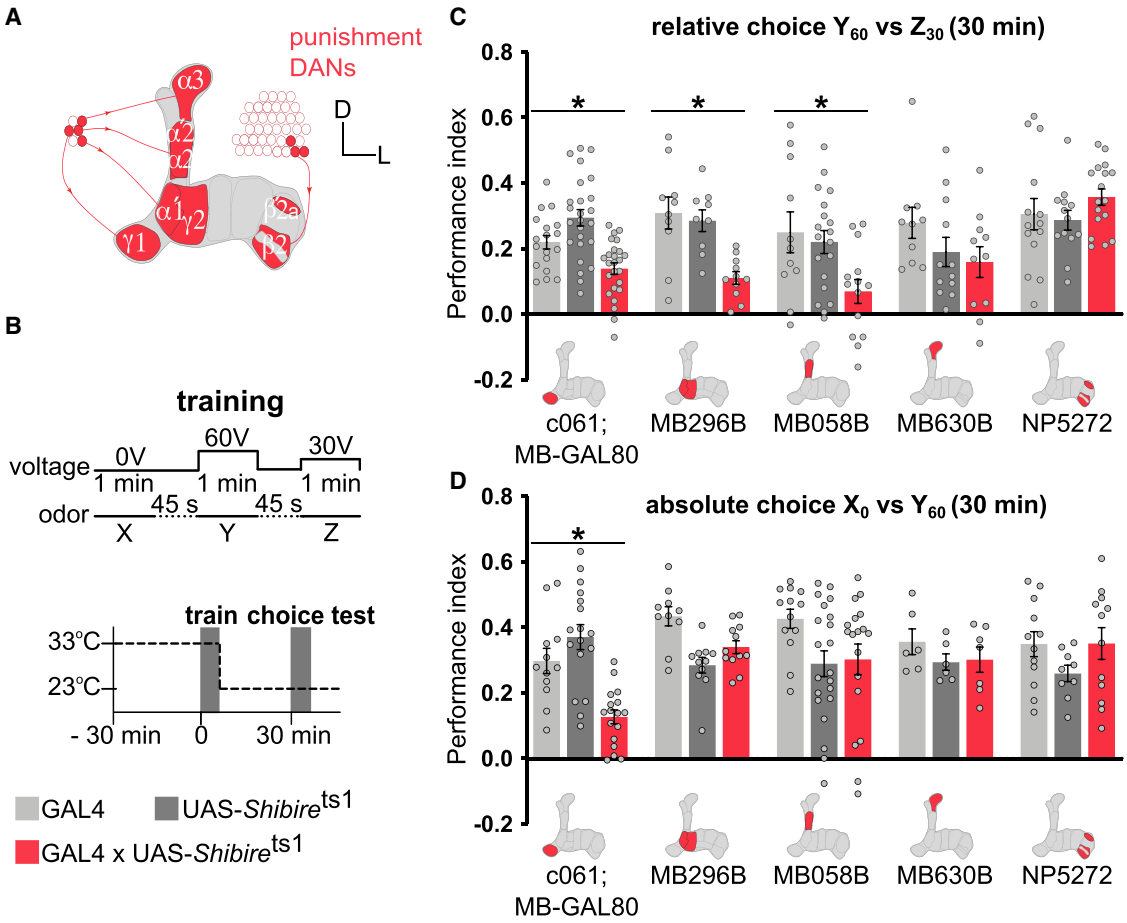

Figure 4. PPL1-γ1pedc, PPL1-γ2α′1, and PPL1-α2α′2 DANs are required to learn relative aversive value, while only PPL1-γ1pedc is necessary to learn absolute aversive value

(A) Schematic of MB innervation by aversively reinforcing DANs.

(B) Training protocol and temperature shifting procedure for *Shi*^{ts1} manipulations.

(C) Blocking output from c061;MBGAL80- (PPL1-γ1pedc), MB296B- (PPL1-γ2α′1), and MB058B- (PPL1-α2α′2) but not MB630B- (PPL1-α3) or NP5272- (PAM-β2β′2a) GAL4 neurons during training impaired 30 min relative choice, compared with that of relevant controls (one-way ANOVA, n = 18–25, $p < 0.05$; one-way ANOVA, n = 9–11, $p < 0.05$; one-way ANOVA, n = 11–19, $p < 0.05$; Kruskal-Wallis, n = 10–12, $p > 0.05$; one-way ANOVA, n = 13–17, $p > 0.05$, respectively). Data are mean ± SEM. Individual data points are displayed as dots. * $p < 0.05$.

(D) Blocking output from c061;MBGAL80- (PPL1-γ1pedc) but not from MB296B- (PPL1-γ2α′1), MB058B- (PPL1-α2α′2), MB630B- (PPL1-α3), or NP5272- (PAM-β2β′2a) GAL4 neurons during training impaired 30 min absolute choice, compared with that of relevant controls (one-way ANOVA, n = 12–17, $p < 0.05$; Kruskal-Wallis, n = 10–12, $p > 0.05$; one-way ANOVA, n = 13–21, $p > 0.05$; Kruskal-Wallis, n = 6–7, $p > 0.05$; one-way ANOVA, n = 9–12, $p > 0.05$, respectively). Data are mean ± SEM. Individual data points are displayed as dots. * $p < 0.05$.

See also Figure S4 and Table S1.

S5C) during learning and then gave flies a relative odor choice 30 min after training (Figure 5B). Blocking 0104-GAL4 and R56H09-GAL4, but not 0279-GAL4, DANs only during learning significantly impaired relative choice test performance (Figure 5C). Importantly, control experiments performed at permissive 23°C did not reveal significant differences between the relevant groups (Figure S5L). In addition, these subsets of reward DANs were not required during learning when flies were given an absolute choice, suggesting that both olfactory and shock perception were unaffected by the manipulations (Figure S5M). We next assessed whether subsets of reward DANs, included in the broad reward DAN R58E02-GAL4 (Figure 3B) but not in R56H09-GAL4, were involved in relative aversive value coding. We generated a R56H09-GAL80 line and combined it with R58E02-GAL4 to restrict *Shi*^{ts1} expression to the remaining DANs (Figure S5D). These remaining DANs were not required during learning for either relative (Figure 5C) or absolute (Figure S5M) choice performance.

We used specific GAL4 driver lines to assess the role in learning relative aversive value of individual rewarding DAN subtypes labeled by R56H09-GAL4 (Figures 5C and S5E–S5J). Blocking output of these subtypes with *Shi*^{ts1} only revealed a requirement for β′2aγ5n reward DANs (targeted by MB109B-GAL4) to learn relative aversive value (Figure 5C). Control experiments at permissive 23°C showed no statistical differences between the groups (Figure S5L). As expected, none of these reward DAN subtypes were required during learning for absolute choice (Figure S5M). We also tested a second GAL4 line (MB087C-GAL4) that labels fewer DANs innervating the β′2a

Please cite this article in press as: Villar et al., Differential coding of absolute and relative aversive value in the *Drosophila* brain, Current Biology (2022), https://doi.org/10.1016/j.cub.2022.08.058

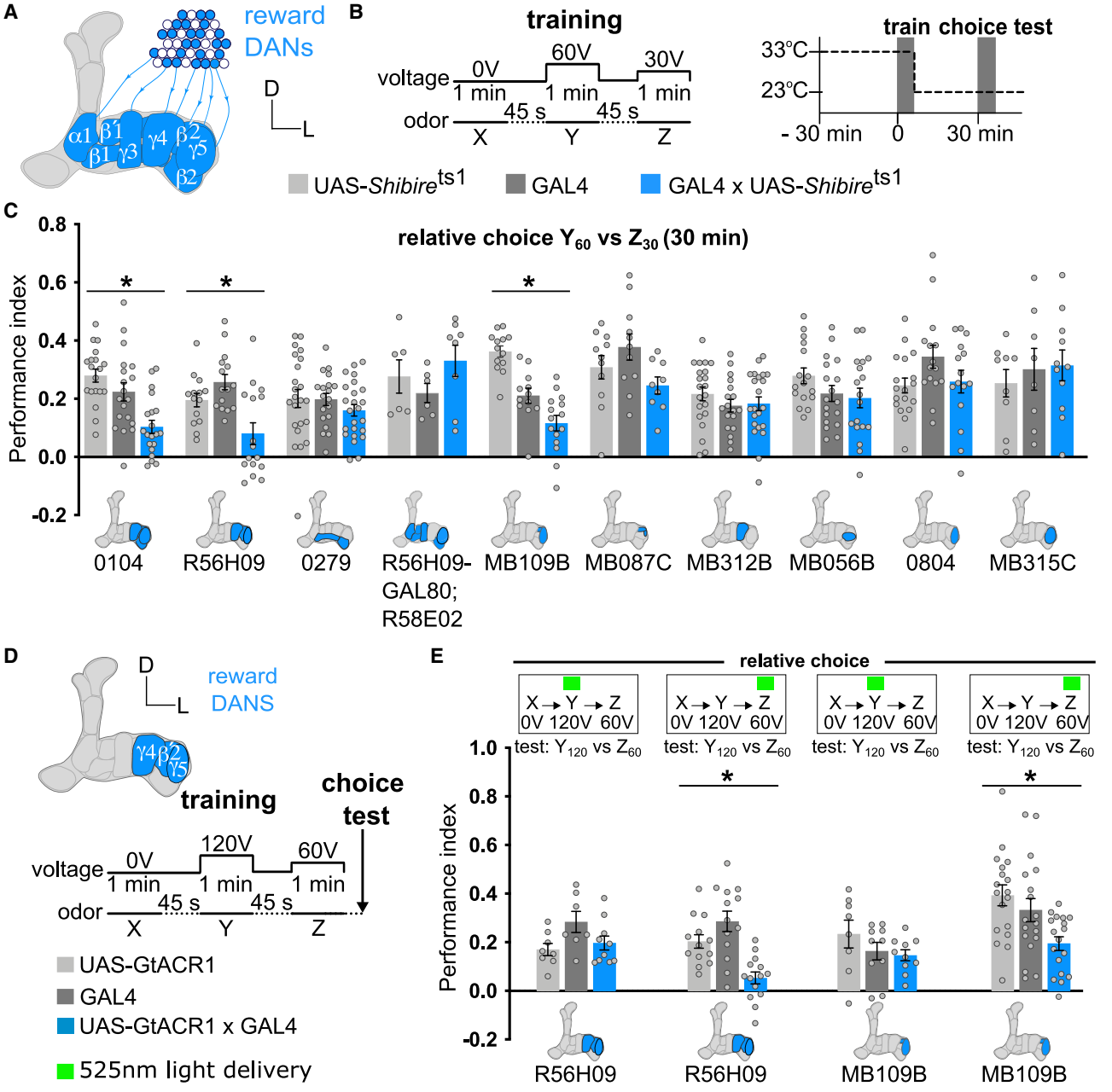

Figure 5. PAM-β′2aγ5n DANs are required to learn relative aversive value

(A) Schematic of MB innervation of reward DANs.

(B) Training protocol and temperature shifting procedure for *Shi*^{ts1} manipulations.

(C) Blocking output from 0104-, R56H09-, and MB109B-GAL4 but not from 0279-, R56H09-GAL80;R58E02-, MB087C-, MB312B-, MB056B-, 0804-, or MB315C-GAL4-targeted PAM DANs during training impaired 30 min relative choice, compared with that of relevant controls (one-way ANOVA, n = 19–20, $p < 0.05$; one-way ANOVA, n = 14–16, $p < 0.05$; one-way ANOVA, n = 12–15, $p < 0.05$; one-way ANOVA, n = 19–24, $p > 0.05$; Kruskal-Wallis, n = 6–8, $p > 0.05$; one-way ANOVA, n = 9–11, $p > 0.05$; one-way ANOVA, n = 18–22, $p > 0.05$; one-way ANOVA, n = 16–18, $p > 0.05$; one-way ANOVA, n = 15–18, $p > 0.05$; one-way ANOVA, n = 8–11, $p > 0.05$, respectively). Data are mean ± SEM. Individual data points are displayed as dots. * $p < 0.05$.

(D) Schematic of reward DAN innervation for R56H09- and MB109-GAL4 and training protocol for optogenetic experiments.

(E) Inhibiting reward DANs with a 525 nm green light exposure only during the last odor Z + 60 V association impaired immediate relative choice (one-way ANOVA, n = 13–14, $p < 0.05$ for R56H09-GAL4 and one-way ANOVA, n = 18, $p < 0.05$ for MB109B-GAL4), but not when inhibited during the odor Y + 120 V association (Kruskal-Wallis, n = 7–10, $p > 0.05$ for R56H09-GAL4 and one-way ANOVA, n = 8–10, $p > 0.05$ for MB109B-GAL4). Data are mean ± SEM. Individual data points are displayed as dots. * $p < 0.05$.

See also Figure S5 and Table S1.

Please cite this article in press as: Villar et al., Differential coding of absolute and relative aversive value in the *Drosophila* brain, Current Biology (2022), https://doi.org/10.1016/j.cub.2022.08.058

CellPress
OPEN ACCESS

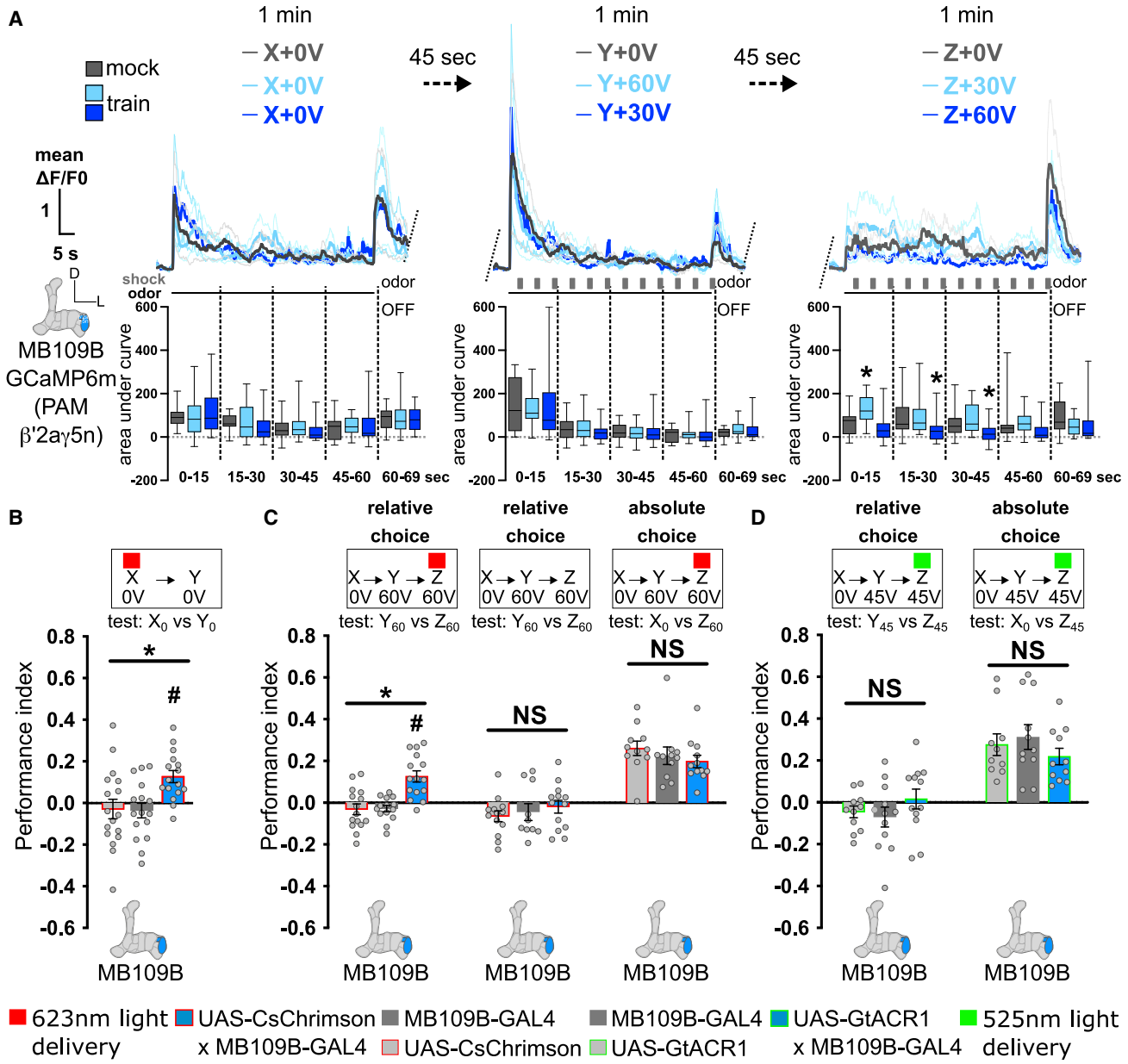

Figure 6. PAM-β′2aγ5n DANs signal a relative "better than" aversive value during learning

(A) Schematic of the MB innervation of recorded PAM-β′2aγ5n (MB109B-GAL4 driving UAS-GCaMP6m, blue). PAM-β′2aγ5n DAN calcium traces and mean area under curve ± SEM quantifications for each 15 s quarter of every 1 min odor presentation for the control mock (X + 0 V, Y + 0 V, and Z + 0 V, black, n = 19) and shock trained (X + 0 V, Y + 60 V, and Z + 30 V, light blue, n = 20; X + 0 V, Y + 30 V, and Z + 60 V, dark blue, n = 17) protocols. All unpaired t test (or Mann-Whitney) compared with mock control. * $p > 0.05$.

(B) Protocol: the first odor X is paired with the optogenetic activation (623 nm light stimulation) of PAM-β′2aγ5n (MB109B-GAL4-driven UAS-CsChrimson) for 1 min. 45 s later, the odor Y is presented for 1 min unpaired. 1 min after training, flies are tested in a T-maze for choice between the odors X_0 versus Y_0. The Performance Index shows fly preferences toward the odor X. one-way ANOVA, n = 16–17, $p < 0.05$ (*); one-sample t test versus 0; #$p < 0.05$.

(C) Flies are trained to associate three odors (X, Y, and Z) paired with 0, 60, and 60 V, respectively. During the last odor Z + 60 V presentation, a 623 nm light stimulation activates PAM-β′2aγ5n DANs (MB109B-GAL4 driving UAS-CsChrimson). 1 min after training, flies are tested in a T-maze for choice between odors Y_{60} versus Z_{60} (relative choice) or X_0 versus Z_{60} (absolute choice). Performance Index shows fly preferences toward the odor Z. During the relative choice, flies preferentially and significantly chose the odor Z_{60} (over the odor Y_{60}), compared with that of genetic background controls (one-way ANOVA, n = 15, $p < 0.05$(*)). One-sample t test versus 0; #$p < 0.05$. Not delivering the 623 nm light stimulation during the odor Z + 60 V presentation had no effect on fly relative choice (one-way ANOVA, n = 10–13, $p > 0.05$). Activating PAM-β′2aγ5n DANs during the odor Z_{60} had no effect on the absolute X_0 versus Z_{60} choice (one-way ANOVA, n = 11–12, $p > 0.05$). Data are mean ± SEM. Individual data points are displayed as dots. * $p < 0.05$.

(D) Flies are trained to associate three odors (X, Y, and Z) paired with 0, 45, and 45 V, respectively. During the last odor Z + 45 V presentation, a 525 nm light stimulation inhibited PAM-β′2aγ5n DANs (MB109B-GAL4 driving UAS-GtACR1). 1 min after training, flies were tested in a T-maze for choice between the odors

(legend continued on next page)

Please cite this article in press as: Villar et al., Differential coding of absolute and relative aversive value in the *Drosophila* brain, Current Biology (2022), https://doi.org/10.1016/j.cub.2022.08.058

and γ5n compartments than are labeled in MB109B-GAL4 (Figures S5F and S5K). Blocking output of MB087C-GAL4 neurons during learning did not alter relative or absolute choices (Figures 5C and S5M). Since all flies exhibited normal absolute choices (Figure S5M), we conclude that both olfactory and shock perception remained intact from the thermogenetic manipulations during training. Together, these results show that particular (or a critical number of) PAM-β′2aγ5n reward DANs are necessary to learn relative aversive value and therefore enable appropriate relative value based choice.

To signal a relative "better than" aversive value during learning, the PAM-β′2aγ5n DANs should only be necessary during the last lesser 30 V experience, when a comparison can be made between current odor Z + 30 V and previous odor Y + 60 V aversive experiences. However, the temporal resolution afforded by thermogenetic *Shi*^{ts1} is not adequate to easily test this hypothesis. We therefore used optogenetics to inhibit rewarding DAN activity during specific segments of the learning session. In addition, classical shock training chambers (as used in all prior experiments) contain copper wires, which decrease light penetrance and impede the use of optogenetics. We therefore designed a transparent shock grid in which conductive indium tin oxide is coated on plastic and can be wrapped inside the training chamber, inspired by a prior apparatus for electric shock-reinforced visual learning.[79] Due to the higher electrical resistance of this material, we altered the training voltages to achieve a similar efficiency of training. Thus, the three different odors (X, Y, and Z) were respectively paired with 0, 120, and 60 V shocks (Figure 5D). During the second or the third odor/shock association, we delivered light with a spectrum peaking at 525 nm to the flies to inhibit the targeted reward DANs (R56H09-GAL4 or MB109B-GAL4) expressing the green light-sensitive anion channelrhodopsin GtACR1.[80] Strikingly, reward DANs were only required during the last training segment (Z + 60 V), being dispensable during the second training segment (Y + 120 V), to enable an appropriate relative choice (Figure 5E). Control experiments without light stimulation showed no differences in the 1 min relative choice test (Figure S5N). Moreover, reward DANs were not needed during the second or third odor/shock association to enable appropriate absolute (X_0 versus Y_{120} or X_0 versus Z_{60}) choices (Figure S5N). These results suggest that the PAM-β′2aγ5n reward DANs are crucial to learn a relative "better than" aversive value between current and previous aversive experiences.

PAM-β′2aγ5n DANs integrate MBON-γ2α′1 input to signal relative aversive value

To potentially visualize a relative "better than" reward value signal, we expressed GCaMP6m and recorded calcium transients from PAM-β′2aγ5n DANs while training flies with the relative aversive value protocol under a two-photon microscope (Figure 6A). We used a mock training protocol as a control, where the same odor presentations were given as in relative aversive training, but no shocks were delivered. Data were analyzed by dividing the recordings made during each 1 min X, Y, and Z odor presentation into four consecutive 15 s segments plus a 9 s segment corresponding to the odor OFF response. No differences were apparent in PAM-β′2aγ5n DAN calcium responses in trained flies (light blue) compared with those of the mock controls (dark gray) during the first odor X, or second odor Y with high 60 V shocks, presentations (Figure 6A). However, we observed a significant elevation of PAM-β′2aγ5n responses in the first quarter of recordings when the last odor Z was presented with lesser 30 V shocks (Figure 6A). In addition, we noted that elevated PAM-β′2aγ5n DAN responses occurred after the first of the 30 V shocks was delivered. The increased PAM-β′2aγ5n DAN response during learning does not result from a simple increase in a 30 V shock-driven response after receiving 60 V shocks (Figure S6). Combined with our behavioral results in Figure 5E, these data are consistent with a model where PAM-β′2aγ5n DANs compare previous and current aversive experience to signal a relative aversive "better than" reward signal during learning, which subsequently supports an appropriate relative value-based odor choice.

To challenge this hypothesis, we tested whether forced activation of PAM-β′2aγ5n DANs could assign a "better than" value to one of two identical aversive experiences. We first demonstrated that pairing artificial activation of PAM-β′2aγ5n DANs with an odor was rewarding (Figure 6B).[49] We next trained flies with the first odor X unpaired (X + 0 V) followed by odor Y paired with 60 V and a third odor Z also paired with 60 V. During this protocol, we optogenetically activated (with light stimulation of UAS-CsChrimson[81]) the PAM-β′2aγ5n DANs during the last odor Z + 60 V pairing (Figure 6C) to potentially mimic a relative "better than" value signal. Flies were then immediately given a Y_{60} versus Z_{60} choice. Whereas control flies showed no preference between the two odors, experimental flies clearly preferred the odor previously paired with 60 V and PAM-β′2aγ5n DAN activation (Figure 6C), demonstrating that they consider the last experience (odor Z + 60 V + DAN supplementation) better than that prior (odor Y + 60 V). Moreover, omitting PAM-β′2aγ5n DAN artificial activation during the last odor Z + 60 V did not alter the immediate relative choice test Y_{60} versus Z_{60} (Figure 6C). Importantly, activating PAM-β′2aγ5n DANs during the last odor Z + 60 V did not affect absolute choice X_0 versus Z_{60} (Figure 6C). We conclude that increased PAM-β′2aγ5n DANs activity during learning signals a relative "better than" value.

Flies can also learn a relative "worse than" aversive value.[8] We therefore reversed the order of the 60 V and 30 V paired odor exposures in our protocol so that the odor Y + 30 V was now delivered before the odor Z + 60 V to investigate neural mechanisms of "worse than" coding (Figure 6A). Imaging PAM-β′2aγ5n DAN calcium responses in trained flies (dark blue) revealed no differences compared with those of the mock controls (dark gray) during the first odor X + 0V or second odor Y + low 30 V shocks. However, a significant decrease of PAM-β′2aγ5n responses was apparent within the second and third quarters of the recordings when the last odor Z was presented with higher 60 V shocks.

Y_{45} versus Z_{45} (relative choice) or X_0 versus Z_{45} (absolute choice). Performance Index shows fly preferences toward the odor Y (left) or X (right). Inhibiting PAM-β′2aγ5n DANs during the odor Z_{45} had no effect on relative (one-way ANOVA, n = 11–12, $p > 0.05$) or absolute choice (one-way ANOVA, n = 10–11, $p > 0.05$). Data are mean ± SEM. Individual data points are displayed as dots.
Also see Figures S6 and S7 and Table S1.

Please cite this article in press as: Villar et al., Differential coding of absolute and relative aversive value in the *Drosophila* brain, Current Biology (2022), https://doi.org/10.1016/j.cub.2022.08.058

CellPress
OPEN ACCESS

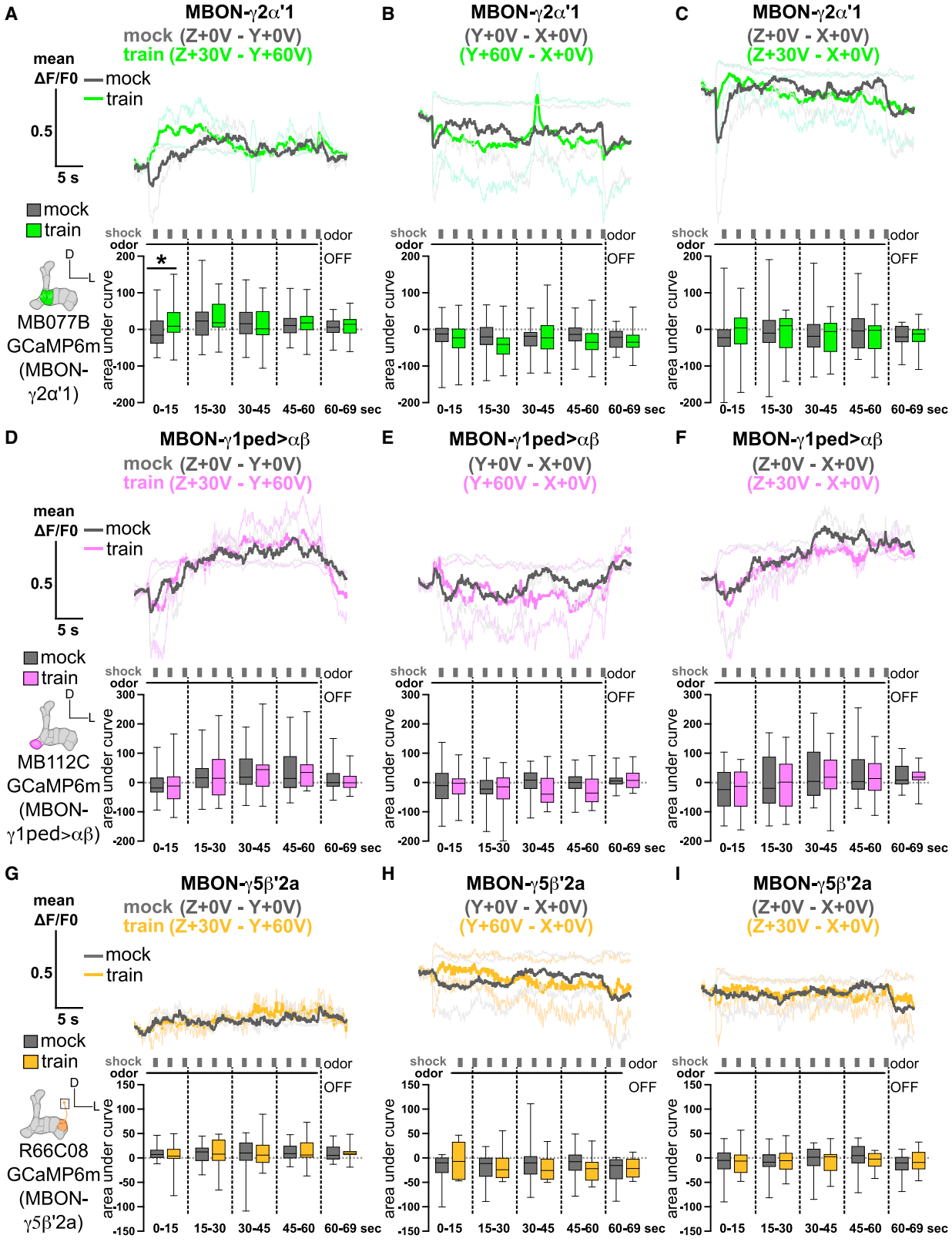

(legend on next page)

Please cite this article in press as: Villar et al., Differential coding of absolute and relative aversive value in the *Drosophila* brain, Current Biology (2022), https://doi.org/10.1016/j.cub.2022.08.058

This decreased PAM-β′2aγ5n DAN response during learning does not result from a change in a 60 V shock-driven signal following 30 V shocks (Figure S6). A relative "worse than" aversive value therefore seems to be associated with inhibition of PAM-β′2aγ5n DANs. To challenge this hypothesis, we trained flies by presenting the first odor X unpaired (X + 0 V) followed by odor Y paired with 45 V and a third odor Z also paired with 45 V. We optogenetically inhibited PAM-β′2aγ5n DANs (with light stimulation peaking at 525 nm to trigger UAS-GtACR1[81]) during the last odor Z + 45 V presentation to mimic a potential relative "worse than" value signal (Figure 6D). We chose 45 V as baseline punishment in this experiment so that we could register "worse than" aversive value, since earlier work indicates that aversive memory performance plateaus above 60 V (Figure 1B).[8,69,70,73] Artificially inhibiting PAM-β′2aγ5n DANs during the last odor Z + 45 V did not alter the immediate relative choice between Y_{45} versus Z_{45} or the absolute choice X_0 versus Z_{45} (Figure 6D). Therefore, signaling a relative "worse than" aversive value may involve inhibition of PAM-β′2aγ5n DANs, but that alone is insufficient to sway valuation between two odors Y_{45} versus Z_{45} that are given equal aversive shock. More work will be required to understand relative "worse than" coding.

To understand how PAM-β′2aγ5n DANs integrate and compare previous and current aversive experience to signal a relative "better than" aversive value, we considered their synaptic input connectivity in the MB network. Strikingly, PAM-β′2aγ5n DANs receive direct synaptic input from MBON-γ2α′1[49,55] and likely fewer inputs from MBON-γ1ped>αβ,[55] both of whose odor-evoked responses are modified by aversive learning (Figures 2 and S2). MBON-γ5β′2a also connects to PAM-β′2aγ5n DANs in recurrent connections,[78] and their odor-evoked responses are potentiated by aversive learning.[47,53,63,64] We made independent recordings from these three MBONs during the relative aversive training protocol (Figure S7). No obvious differences in these MBON odor-evoked responses were apparent during each of the three odor sequences (X + 0 V, Y + 60 V, and Z + 30 V), as compared with flies presented with the mock training protocol (Figures S7A–S7C). Since our model proposes that PAM-β′2aγ5n DANs might compare current and previous aversive experiences coded in each MBON during the last odor Z + 30 V association to signal a relative "better than" aversive value, we subtracted the (previous) odor-evoked responses during the odor Y + 60 V association from those during the (current) odor Z + 30 V association. This analysis uncovered a significant increase in the differential responses of MBON-γ2α′1 during the first quarter (the first 3 shocks) of the odor/shock training sessions, as compared with those in flies subjected to mock training (Figure 7A). Importantly, and as with PAM-β′2aγ5n DANs, this differential increased response was evident after the first of the 30 V shocks was delivered. By contrast, subtractive analyses did not reveal any differences between present (Z + 30 V) and prior (Y + 60 V) responses for MBON-γ1ped>αβ or MBON-γ5β′2a (Figures 7D and 7G). In addition, no statistical differences were evident for any MBON when we subtracted the odor-evoked response during the odor Y + 60 V association from those during the first unpaired odor X + 0 V presentation (Figures 7B, 7E, and 7H) and the subtraction of odor-evoked response during the odor Z + 30 V association from those during the first unpaired odor X + 0 V presentation (Figures 7C, 7F, and 7I).

Figure 7. MBON-γ2α′1, but neither MBON-γ1ped>αβ nor MBON-γ5β′2a, exhibits differential responses between trained odors during training

(A) Schematic of the MB innervation of recorded MBON-γ2α′1 (MB077B-GAL4 driving UAS-GCaMP6m, green). Mean subtracted Z + 30 V – Y + 60 V calcium traces and quantifications of mean area under the curve of MBON-γ2α′1 during the training (n = 23) and mock (n = 26) protocols. A significant increase was only found during the first quarter of the odor presentation period in the Z + 30 V – Y + 60 V subtracted responses of the trained group, compared with that of the mock group (unpaired t test; * $p < 0.05$). All other comparisons are non-significant (unpaired t or Mann-Whitney tests; $p > 0.05$).

(B) Mean subtracted Y + 60 V – X + 0 V calcium traces and mean area under curve of MBON-γ2α′1 during the training (n = 23) and mock (n = 26) protocols. We found no significant differences during the odor presentation subtraction Y + 60 V – X + 0 V between trained and mock groups (unpaired t and Mann-Whitney tests; $p > 0.05$).

(C) Mean subtracted Z + 30 V – X + 0 V calcium traces and mean area under curve of MBON-γ2α′1 during the training (n = 23) and mock (n = 26) protocols. We found no significant differences during the odor presentation subtraction Z + 30 V – X + 0 V between trained and mock groups (unpaired t and Mann-Whitney tests; $p > 0.05$).

(D) Schematic of the MB innervation of recorded MBON-γ1ped>αβ (MB112C-GAL4 driving UAS-GCaMP6m, magenta). Mean subtracted Z + 30 V – Y + 60 V calcium traces and mean area under curve for MBON-γ1ped>αβ during mock (n = 21) or shock training (n = 21) protocols. We found no significant differences during the odor presentation subtraction Z + 30 V – Y + 60 V between trained and mock groups (all unpaired t or Mann-Whitney tests; $p > 0.05$).

(E) Mean subtracted Y + 60 V – X + 0 V calcium traces and mean area under the curve of MBON-γ1ped>αβ during mock (n = 21) or shock training (n = 21) protocols. We found no significant differences during the odor presentation subtraction Y + 60 V – X + 0 V between trained and mock groups (all unpaired t or Mann-Whitney tests; $p > 0.05$).

(F) Mean subtracted Z + 30 V – X + 0 V calcium traces and mean area under curve of MBON-γ1ped>αβ during the training (n = 21) and mock (n = 21) protocols. We found no significant differences during the odor presentation subtraction Z + 30 V – X + 0 V between trained and mock groups (unpaired t and Mann-Whitney tests; $p > 0.05$).

(G) Schematic of the MB innervation of recorded MBON-γ5β′2a (R66C08-GAL4 driving UAS-GCaMP6m, orange). Mean subtracted Z + 30 V – Y + 60 V calcium traces and mean area under the curve for MBON-γ5β′2a during mock (n = 14) or shock training (n = 11) protocols. We found no significant differences during the odor presentation subtraction Z + 30 V – Y + 60 V between trained and mock groups (all unpaired t or Mann-Whitney tests; $p > 0.05$).

(H) Mean subtracted Y + 60 V – X + 0 V calcium traces and mean area under the curve for MBON-γ5β′2a during mock (n = 14) or shock training (n = 11) protocols. We found no significant differences during the odor presentation subtraction Y + 60 V – X + 0 V between trained and mock groups (all unpaired t or Mann-Whitney tests; $p > 0.05$).

(I) Mean subtracted Z + 30 V – X + 0 V calcium traces and mean area under curve of MBON-γ1ped>αβ during the training (n = 14) and mock (n = 11) protocols. We found no significant differences during the odor presentation subtraction Z + 30 V – X + 0 V between trained and mock groups (unpaired t and Mann-Whitney tests; $p > 0.05$).

See also Figure S7 and Table S1.

Please cite this article in press as: Villar et al., Differential coding of absolute and relative aversive value in the *Drosophila* brain, Current Biology (2022), https://doi.org/10.1016/j.cub.2022.08.058

Altogether, we propose that comparing a difference between a low shock (current) and a high shock (previous) aversive experience requires additional cholinergic input from MBON-γ2α′1 to trigger the PAM-β′2aγ5n DANs, which signal a relative "better than" aversive value to the lesser aversive olfactory experience.

DISCUSSION

Our study addresses how animals assign absolute aversive value during learning and how they compare and ascribe relative aversive value information to consecutive negative experiences for them to make appropriate value-based decisions afterwards. Using the fruit fly *Drosophila* permitted a cellular resolution view of how the interaction between the appetitive and aversive DAN systems, within the MB network, is at the heart of the mechanistic underpinnings that compute a relative aversive value teaching signal. Our work also indicates that coding of a relative "worse than" aversive value likely involves different circuit mechanisms to those for "better than" but that there may be some overlap.

Aversive experience is uniquely coded at the KC-MBON-γ1ped>αβ and -MBON-γ2α′1 junctions

PPL1 DANs reinforce a range of aversive memories with differing strength and persistence.[37–39,41,57,62,82,83] Our data provide new insight into the functional diversity of these anatomically discrete DANs (Figures 1, 3, 4, S1, S3, and S4). We found that individual aversively reinforcing PPL1-γ1pedc, PPL1-γ2α′1, and PPL1-α2α′2 DANs exhibit different intensity response profiles when flies were exposed to a series of shock voltages.[74,75] Importantly, the strength of their responses to electric shocks strongly correlated with the magnitude of plasticity of the odor-evoked responsiveness of their corresponding MBONs after differential conditioning (Figures 1, 2, S1, and S2). These results indicate that absolute aversive value is assigned to odors in different ways in the γ1pedc, γ2α′1, and α2α′2 MB compartments, consistent with the conclusion of a prior study that artificially activated individual DANs.[62] Of note, we did not observe significant shock responses in PPL1-α2α′2 DANs (Figures 1H and 1I). These results are also in accordance with the absence of odor-evoked changes in the corresponding MBON-α2sc immediately after training (Figures 2G and 2H) and a lack of reinforcing properties when pairing artificial activation of PPL1-α2α′2 DANs with an odor[40] (but see Hige et al.[62]). In addition, learning-dependent depression of odor responses in MBON-α2sc has been reported to be most relevant for expression of later forms of memory.[60,64] We observed that the stronger the aversive experience, the greater the PPL1-γ1pedc DAN-driven depression of the CS+-evoked response of MBON-γ1ped>αβ (Figures 2C, 2D, S2D, and S2E). Feedforward GABAergic inhibition from MBON-γ1ped>αβ to the primary axon of MBON-γ5β′2a[47,53] is therefore reduced in a graded manner by aversive conditioning. MBON-γ5β′2a should therefore display a proportional increase in its CS+-evoked response to drive learned avoidance behavior.[63,64] Our experiments uncovered a very different effect of absolute aversive conditioning at the MBON-γ2α′1 junction. Although the PPL1-γ2α′1 DANs were significantly triggered by shocks ≥30 V, their responses were comparable at all voltages between 30 and 90 V (Figures 1F and 1G). Moreover, aversive conditioning did not significantly depress the CS+ responses of MBON-γ2α′1 (Figures 2E, 2F, S2F, and S2G). Instead, we observed that the responses to the CS− odor were specifically increased, and the CS− CS+ differential responses were correlated with the intensity of the shocks applied (Figures 2J and S2I) (these results differ from those of Berry et al.,[65] perhaps due to a different response comparison). Our data therefore suggest that any odor that follows the CS+ with ≥45 V presentation during training gains the capacity to drive more activity in the cholinergic MBON-γ2α′1. In addition, our recordings indicate that the more aversive the first experience is, the stronger the cholinergic MBON-γ2α′1 activity will be to the subsequent "better than" experience. These data reveal a key role for MBON-γ2α′1 in coding relative aversive value.

MBON-γ2α′1 input to PAM-β′2aγ5n DANs provides a "better than" reward signal during relative aversive training

We found that output from PAM-β′2aγ5n DANs was critical during the odor Z + 30 V presentation for relative aversive learning (Figure 5). These DANs receive direct excitatory cholinergic input from MBON-γ2α′1,[49,55] and we propose that the strength of this excitation is key for the flies to assign a "better than" reward value to the lesser of the two aversive experiences. As mentioned above, when odor Y is paired with 60 V shock in a differential conditioning assay, the CS− responses of MBON-γ2α′1 become elevated. This means that when Y + 60 V is followed by Z + 30 V, the Z odor will more strongly drive MBON-γ2α′1 and as a result will activate the PAM-β′2aγ5n DANs (Figure 6A). In effect, we hypothesize that any odor that follows a Y + 60 V experience is predisposed to be judged as "better than," unless it is itself accompanied by 60 V or a greater voltage. Our analyses that subtracted MBON-γ2α′1 odor-evoked responses are entirely consistent with this model. Odor-driven activity of MBON-γ2α′1 is greater during the first period of the following Z + 30 V experience than during the same period (just after the first shock) of the prior Y + 60 V experience (Figure 7A). Critically, this is also the time period during which we observed an elevation of PAM-β′2aγ5n DAN activity (Figure 6A). We speculate that the first of the 30 V shocks somehow further releases the PAM-β′2aγ5n DAN activity to be fully driven by MBON-γ2α′1, perhaps as a release of feedforward inhibition in the MBON-γ1ped>αβ to MBON-γ5β′2a to PAM-β′2aγ5n DAN pathway.[47,53] Our results (Figure 6B) and proposed models of PAM-β′2aγ5n DANs providing a "better than" reward signal are in accordance with previous reports that PAM-β′2aγ5n activation provides appetitive reinforcement.[40,44,49,84]

Are there limits to comparable aversive memories?

Individual PPL1-DAN subtypes have different thresholds for activation, and intensity-dependent plasticity in their corresponding MBON junctions have similar thresholds. We noted that these thresholds seem reflected in the range of comparisons that flies can make in a relative choice between different aversive memories,[8] which point toward a threshold and a difference between voltages of 30 V as being optimal to efficiently estimate a relative difference. In our recordings (Figure 1), 30 V was the threshold for observing shock-evoked responses in PPL1-γ1pedc and PPL1-γ2α′1, but it did not trigger PPL1-α2α′2. In addition, 30 V produced significant plasticity of MBON-γ1ped>αβ odor

Please cite this article in press as: Villar et al., Differential coding of absolute and relative aversive value in the *Drosophila* brain, Current Biology (2022), https://doi.org/10.1016/j.cub.2022.08.058

responses, but plasticity was not evident in MBON-γ2α′1 responses until 45 V. Thus, perhaps every odor paired with a voltage of ≤30 V is considered to be "not so bad," because it only depresses the GABAergic MBON-γ1ped>αβ responses and not the cholinergic MBON-γ2α′1 responses, thereby leaving CS+ odor-driven excitation of PAM-β′2aγ5n DANs from these MBONs. Although flies can differentiate between stronger aversive memories such as 90 versus 60 V, their relative choice performances are less good than 60 versus 30 V.[8] While we did not observe significant shock responses for PPL1-α2α′2 DANs, we found a role for these neurons during learning of relative aversive value (Figure 4). MBON-γ1ped>αβ is GABAergic and is connected to PPL1-α2α′2 DANs.[41,55] It is therefore possible that repeated pairing of odor Y + 60 V electric shocks (or anything above their threshold) during relative training induces enough CS+-evoked depression at MBON-γ1ped>αβ to release inhibition in PPL1-α2α′2 DANs while pairing the odor Z with 30 V shocks.[85,86] The resulting plasticity in MBON-α2sc could explain the requirement of αβ surface and αβ core KCs during a relative choice between Y_{60} versus Z_{30}.[21]

Relative evaluation of aversive experiences

Our results show that learning a relative "better than" aversive value requires an interplay between aversively reinforcing PPL1 DANs modulating KC-MBON connections, which provide feedforward and recurrent feedback input that determines the activity of specific subtypes of rewarding PAM DANs. These results support long-held[87,88] and recent[47–49,58,89,90] models in both vertebrates and invertebrates, suggesting that learning requires critical interactions between appetitive and aversive reinforcement systems. In the fly, and likely also in mammals, this process relies on opposing populations of DANs providing predictive signals needed to compare current and previous experience to assign (and update) both absolute and relative value to stimuli during learning. For instance, aversive memory extinction and reversal learning require the reward system in both vertebrates and invertebrates.[47,90–92] In all these cases, stimuli that represent the absence of a punishment are rewarded.[47,49,93] In humans, the ventral striatum, targeted by numerous DA inputs from the ventral tegmental area (VTA) providing rewarding information, is essential to compare aversive experiences of different intensities.[20,31] In the orbitofrontal cortex, relative coding of aversive (but also appetitive) experiences seem to require overlapping neuronal ensembles to select a preferred option and promote appropriate economical decisions in a specific spatial and temporal context.[3,17,22,94] In the dopaminergic system, reward is also computed in a relative manner to broadcast value signals in different brain regions.[10] These DANs from the VTA and substantia nigra compute a prediction error to signal positive, but also negative, value (for reviews, see Glimcher[27] and Watabe-Uchida et al.[28]). A similar value prediction error calculation has not yet been demonstrated experimentally in the fly.[75,95] Instead, results from several studies in the fly suggest that errors are registered in the MB network by the action of DANs that signal the opposing value.[47–49,96] Our experiments here suggest that a similar interplay between opposing populations of DANs, and plasticity at different MBON junctions in the MB network, permits computation of relative aversive value (or difference) between a prior and a new aversive experience. Combined with previous work[47–49,57,58] and current computational models,[73,97] our data provide key features of how the appetitive-aversive system interactions in the MB network using heterogeneous DANs can compare previous and current experience to "pre-compute" a relative value during learning[5] that facilitates future value-based decisions.

STAR★METHODS

Detailed methods are provided in the online version of this paper and include the following:

- KEY RESOURCES TABLE
- RESOURCE AVAILABILITY
  - Lead contact
  - Materials availability
  - Data and code availability
- EXPERIMENTAL MODEL AND SUBJECT DETAILS
  - Animals
- METHOD DETAILS
  - Fly construct
  - Behavioral Analyses
  - Immunohistochemistry and confocal microscopy
  - *In vivo* two-photon calcium imaging
- QUANTIFICATION AND STATISTICAL ANALYSIS

SUPPLEMENTAL INFORMATION

Supplemental information can be found online at https://doi.org/10.1016/j.cub.2022.08.058.

ACKNOWLEDGMENTS

We thank Stephanie Trouche, Johannes Felsenberg, and Suewei Lin for comments on the manuscript. We thank the Bloomington Stock Center for flies. We thank Yaling Huang for making the R56H09-GAL80 construct. We thank Richard Griffith and Luis D. Suarez for help with behavioral experiments. E.P. is funded by the ATIP-Avenir program from CNRS and Inserm, the Bettencourt Schueller Foundation, the French National Research Agency (ANR-PRC 2021), and the Institute of Functional Genomics, Montpellier, France. S.W. is funded by a Wellcome Trust Principal Research Fellowship in the Basic Biomedical Sciences (200846/Z/16/Z) and a Wellcome Trust Collaborative Award (2023261/Z/16/Z). We thank the Montpellier Biocampus facilities (University of Montpellier, CNRS, INSERM, Montpellier, France) MRI, Drosophila facility, and IPAM for the confocal microscopy, the fly food, and the two-photon microscope, respectively.

AUTHOR CONTRIBUTIONS

E.P. and S.W. conceived the project, and M.V., M.P.-D., and E.P. designed all experiments. E.P., M.V., N.M., and S.A.P. performed behavioral experiments. E.P. and M.V. analyzed all behavioral experiments. M.P.-D., E.P., A.P., P.F.J., and M.A. performed imaging experiments. E.P., M.A., and M.P.-D. analyzed imaging data. Anatomical data were collected by M.V. and E.P. The manuscript was written by E.P., M.V., M.P.-D., and S.W.

DECLARATION OF INTERESTS

The authors declare no competing interests.

Received: March 10, 2022
Revised: June 24, 2022
Accepted: August 19, 2022
Published: September 13, 2022

REFERENCES

1. Rangel, A., Camerer, C., and Montague, P.R. (2008). A framework for studying the neurobiology of value-based decision making. Nat. Rev. Neurosci. *9*, 545–556.
2. Pavlov, I.P. (1927). Conditioned Reflexes (Oxford University Press).
3. Tremblay, L., and Schultz, W. (1999). Relative reward preference in primate orbitofrontal cortex. Nature *398*, 704–708.
4. Seymour, B., and McClure, S.M. (2008). Anchors, scales and the relative coding of value in the brain. Curr. Opin. Neurobiol. *18*, 173–178.
5. Hunter, L.E., and Daw, N.D. (2021). Context-sensitive valuation and learning. Curr. Opin. Behav. Sci. *41*, 122–127.
6. Louie, K., and Glimcher, P.W. (2012). Efficient coding and the neural representation of value. Ann. N. Y. Acad. Sci. *1251*, 13–32.
7. Wendt, S., Strunk, K.S., Heinze, J., Roider, A., and Czaczkes, T.J. (2019). Positive and negative incentive contrasts lead to relative value perception in ants. eLife *8*, 1–22.
8. Yin, Y., Chen, N., Zhang, S., and Guo, A. (2009). Choice strategies in *Drosophila* are based on competition between olfactory memories. Eur. J. Neurosci. *30*, 279–288.
9. Schleyer, M., Weiglein, A., Thoener, J., Strauch, M., Hartenstein, V., Kantar Weigelt, M.K., Schuller, S., Saumweber, T., Eichler, K., Rohwedder, A., et al. (2020). Identification of dopaminergic neurons that can both establish associative memory and acutely terminate its behavioral expression. J. Neurosci. *40*, 5990–6006.
10. Tobler, P.N., Fiorillo, C.D., and Schultz, W. (2005). Adaptive coding of reward value by dopamine neurons. Science *307*, 1642–1645.
11. Padoa-Schioppa, C., and Conen, K.E. (2017). Orbitofrontal cortex: a neural circuit for economic decisions. Neuron *96*, 736–754.
12. Diederen, K.M.J., Ziauddeen, H., Vestergaard, M.D., Spencer, T., Schultz, W., and Fletcher, P.C. (2017). Dopamine modulates adaptive prediction error coding in the human midbrain and striatum. J. Neurosci. *37*, 1708–1720.
13. Padoa-Schioppa, C., and Assad, J.A. (2006). Neurons in the orbitofrontal cortex encode economic value. Nature *441*, 223–226.
14. Lim, S.L., O'Doherty, J.P., and Rangel, A. (2011). The decision value computations in the vmPFC and striatum use a relative value code that is guided by visual attention. J. Neurosci. *31*, 13214–13223.
15. Strait, C.E., Sleezer, B.J., and Hayden, B.Y. (2015). Signatures of value comparison in ventral striatum neurons. PLoS Biol *13*, e1002173.
16. Hebscher, M., Barkan-Abramski, M., Goldsmith, M., Aharon-Peretz, J., and Gilboa, A. (2015). Memory, decision-making, and the ventromedial prefrontal cortex (vmPFC): the roles of subcallosal and posterior orbitofrontal cortices in monitoring and control processes. Cereb Cortex *26*, 4590–4601.
17. Saez, R.A., Saez, A., Paton, J.J., Lau, B., and Salzman, C.D. (2017). Distinct roles for the amygdala and orbitofrontal cortex in representing the relative amount of expected reward. Neuron *95*, 70–77.e3.
18. Lak, A., Stauffer, W.R., and Schultz, W. (2016). Dopamine neurons learn relative chosen value from probabilistic rewards. eLife *5*, e18044.
19. Klein, T.A., Ullsperger, M., and Jocham, G. (2017). Learning relative values in the striatum induces violations of normative decision making. Nat. Commun. *8*, 16033.
20. Brooks, A.M., Pammi, V.S.C.C., Noussair, C., Capra, C.M., Engelmann, J.B., and Berns, G.S. (2010). From bad to worse: striatal coding of the relative value of painful decisions. Front. Neurosci. *4*, 176.
21. Perisse, E., Yin, Y., Lin, A.C.A., Lin, S., Huetteroth, W., and Waddell, S. (2013). Different kenyon cell populations drive learned approach and avoidance in *drosophila*. Neuron *79*, 945–956.
22. Hosokawa, T., Kato, K., Inoue, M., and Mikami, A. (2007). Neurons in the macaque orbitofrontal cortex code relative preference of both rewarding and aversive outcomes. Neurosci. Res. *57*, 434–445.
23. Campese, V.D., Kim, I.T., Hou, M., Gupta, S., Draus, C., Kurpas, B., Burke, K., and LeDoux, J.E. (2019). Chemogenetic inhibition reveals that processing relative but not absolute threat requires basal amygdala. J. Neurosci. *39*, 8510–8516.
24. Sutton, R.S., and Barto, A.G. (1998). Reinforcement Learning: an Introduction (The MIT Press).
25. Rescorla, R.A., and Wagner, A.R. (1972). A theory of Pavlovian conditioning: Variations in the effectiveness of reinforcement and nonreinforcement. In Classical conditioning: current research and theory, A.H. Black, and W.F. Prokasy, eds. (Appleton-Century-Crofts), pp. 64–99.
26. Schultz, W., Dayan, P., and Montague, P.R. (1997). A neural substrate of prediction and reward. Science *275*, 1593–1599.
27. Glimcher, P.W. (2011). Understanding dopamine and reinforcement learning: the dopamine reward prediction error hypothesis. Proc. Natl. Acad. Sci. USA *108* (*Supplement 3*), 15647–15654.
28. Watabe-Uchida, M., Eshel, N., and Uchida, N. (2017). Neural circuitry of reward prediction error. Annu. Rev. Neurosci. *40*, 373–394.
29. Waddell, S. (2013). Reinforcement signalling in *Drosophila*; dopamine does it all after all. Curr. Opin. Neurobiol. *23*, 324–329.
30. Watabe-Uchida, M., and Uchida, N. (2018). Multiple dopamine systems: weal and woe of dopamine. Cold Spring Harb. Symp. Quant. Biol. *83*, 83–95.
31. Brooks, A.M., and Berns, G.S. (2013). Aversive stimuli and loss in the mesocorticolimbic dopamine system. Trends Cogn. Sci. *17*, 281–286.
32. Adel, M., and Griffith, L.C. (2021). The role of dopamine in associative learning in *drosophila*: an updated Unified Model. Neurosci. Bull. *37*, 831–852.
33. Heisenberg, M. (2003). Mushroom body memoir: from maps to models. Nat. Rev. Neurosci. *4*, 266–275.
34. Waddell, S. (2010). Dopamine reveals neural circuit mechanisms of fly memory. Trends Neurosci *33*, 457–464.
35. Aso, Y., Sitaraman, D., Ichinose, T., Kaun, K.R., Vogt, K., Belliart-Guérin, G., Plaçais, P.Y., Robie, A.A., Yamagata, N., Schnaitmann, C., et al. (2014). Mushroom body output neurons encode valence and guide memory-based action selection in *Drosophila*. eLife *3*, e04580.
36. Schwaerzel, M., Monastirioti, M., Scholz, H., Friggi-Grelin, F., Birman, S., and Heisenberg, M. (2003). Dopamine and octopamine differentiate between aversive and appetitive olfactory memories in *Drosophila*. J. Neurosci. *23*, 10495–10502.
37. Claridge-Chang, A., Roorda, R.D., Vrontou, E., Sjulson, L., Li, H., Hirsh, J., and Miesenböck, G. (2009). Writing memories with light-addressable reinforcement circuitry. Cell *139*, 405–415.
38. Aso, Y., Siwanowicz, I., Bräcker, L., Ito, K., Kitamoto, T., and Tanimoto, H. (2010). Specific dopaminergic neurons for the formation of labile aversive memory. Curr. Biol. *20*, 1445–1451.
39. Aso, Y., Herb, A., Ogueta, M., Siwanowicz, I., Templier, T., Friedrich, A.B., Ito, K., Scholz, H., and Tanimoto, H. (2012). Three dopamine pathways induce aversive odor memories with different stability. PLoS Genet *8*, e1002768.
40. Aso, Y., and Rubin, G.M. (2016). Dopaminergic neurons write and update memories with cell-type-specific rules. eLife *5*, 1–15.
41. Takemura, S.Y., Aso, Y., Hige, T., Wong, A., Lu, Z., Xu, C.S., Rivlin, P.K., Hess, H., Zhao, T., Parag, T., et al. (2017). A connectome of a learning and memory center in the adult Drosophila brain. eLife *6*, 1–43.
42. Liu, C., Plaçais, P.Y., Yamagata, N., Pfeiffer, B.D., Aso, Y., Friedrich, A.B., Siwanowicz, I., Rubin, G.M., Preat, T., and Tanimoto, H. (2012). A subset of dopamine neurons signals reward for odour memory in *Drosophila*. Nature *488*, 512–516.
43. Burke, C.J., Huetteroth, W., Owald, D., Perisse, E., Krashes, M.J., Das, G., Gohl, D., Silies, M., Certel, S., and Waddell, S. (2012). Layered reward signalling through octopamine and dopamine in *Drosophila*. Nature *492*, 433–437.

44. Huetteroth, W., Perisse, E., Lin, S., Klappenbach, M., Burke, C., and Waddell, S. (2015). Sweet taste and nutrient value subdivide rewarding dopaminergic neurons in *drosophila*. Curr. Biol. *25*, 751–758.

45. Yamagata, N., Ichinose, T., Aso, Y., Plaçais, P.Y., Friedrich, A.B., Sima, R.J., Preat, T., Rubin, G.M., and Tanimoto, H. (2015). Distinct dopamine neurons mediate reward signals for short- and long-term memories. Proc. Natl. Acad. Sci. USA *112*, 578–583.

46. Lin, S., Owald, D., Chandra, V., Talbot, C., Huetteroth, W., and Waddell, S. (2014). Neural correlates of water reward in thirsty *Drosophila*. Nat. Neurosci. *17*, 1536–1542.

47. Felsenberg, J., Jacob, P.F., Walker, T., Barnstedt, O., Edmondson-Stait, A.J., Pleijzier, M.W., Otto, N., Schlegel, P., Sharifi, N., Perisse, E., et al. (2018). Integration of parallel opposing memories underlies memory extinction. Cell *175*, 709–722.e15.

48. Jacob, P.F., and Waddell, S. (2020). Spaced training forms complementary long-term memories of opposite valence in *drosophila*. Neuron *106*, 977–991.e4.

49. McCurdy, L.Y., Sareen, P., Davoudian, P.A., and Nitabach, M.N. (2021). Dopaminergic mechanism underlying reward-encoding of punishment omission during reversal learning in *Drosophila*. Nat. Commun. *12*, 1115.

50. Wang, Y., Wright, N.J., Guo, H., Xie, Z., Svoboda, K., Malinow, R., Smith, D.P., and Zhong, Y. (2001). Genetic manipulation of the odor-evoked distributed neural activity in the Drosophila mushroom body. Neuron *29*, 267–276.

51. Honegger, K.S., Campbell, R.A.A., and Turner, G.C. (2011). Cellular-resolution population imaging reveals robust sparse coding in the drosophila mushroom body. J. Neurosci. *31*, 11772–11785.

52. Tanaka, N.K., Tanimoto, H., and Ito, K. (2008). Neuronal assemblies of the *Drosophila* mushroom body. J. Comp. Neurol. *508*, 711–755.

53. Perisse, E., Owald, D., Barnstedt, O., Talbot, C.B., Huetteroth, W., and Waddell, S. (2016). Aversive learning and appetitive motivation toggle feed-forward inhibition in the *drosophila* mushroom body. Neuron *90*, 1086–1099.

54. Hattori, D., Aso, Y., Swartz, K.J., Rubin, G.M., Abbott, L.F., and Axel, R. (2017). Representations of novelty and familiarity in a mushroom body compartment. Cell *169*, 956–969.e17.

55. Li, F., Lindsey, J.W., Marin, E.C., Otto, N., Dreher, M., Dempsey, G., Stark, I., Bates, A.S., Pleijzier, M.W., Schlegel, P., et al. (2020). The connectome of the adult *Drosophila* mushroom body provides insights into function. eLife *9*, 1–217.

56. Aso, Y., Hattori, D., Yu, Y., Johnston, R.M., Iyer, N.A., Ngo, T.T., Dionne, H., Abbott, L.F., Axel, R., Tanimoto, H., and Rubin, G.M. (2014). The neuronal architecture of the mushroom body provides a logic for associative learning. eLife *3*, e04577.

57. Eschbach, C., Fushiki, A., Winding, M., Schneider-Mizell, C.M., Shao, M., Arruda, R., Eichler, K., Valdes-Aleman, J., Ohyama, T., Thum, A.S., et al. (2020). Recurrent architecture for adaptive regulation of learning in the insect brain. Nat. Neurosci. *23*, 544–555.

58. Eschbach, C., Fushiki, A., Winding, M., Afonso, B., Andrade, I.V., Cocanougher, B.T., Eichler, K., Gepner, R., Si, G., Valdes-Aleman, J., et al. (2021). Circuits for integrating learned and innate valences in the insect brain. eLife *10*, 1–36.

59. Cohn, R., Morantte, I., and Ruta, V. (2015). Coordinated and compartmentalized neuromodulation shapes sensory processing in *drosophila*. Cell *163*, 1742–1755.

60. Séjourné, J., Plaçais, P.Y., Aso, Y., Siwanowicz, I., Trannoy, S., Thoma, V., Tedjakumala, S.R., Rubin, G.M., Tchénio, P., Ito, K., et al. (2011). Mushroom body efferent neurons responsible for aversive olfactory memory retrieval in *Drosophila*. Nat. Neurosci. *14*, 903–910.

61. Boto, T., Louis, T., Jindachomthong, K., Jalink, K., and Tomchik, S.M.M. (2014). Dopaminergic modulation of cAMP drives nonlinear plasticity across the *drosophila* mushroom body lobes. Curr. Biol. *24*, 822–831.

62. Hige, T., Aso, Y., Modi, M.N., Rubin, G.M., and Turner, G.C. (2015). Heterosynaptic plasticity underlies aversive olfactory learning in *drosophila*. Neuron *88*, 985–998.

63. Owald, D., Felsenberg, J., Talbot, C.B., Das, G., Perisse, E., Huetteroth, W., and Waddell, S. (2015). Activity of defined mushroom body output neurons underlies learned olfactory behavior in *drosophila*. Neuron *86*, 417–427.

64. Bouzaiane, E., Trannoy, S., Scheunemann, L., Plaçais, P.Y., and Preat, T. (2015). Two independent mushroom body output circuits retrieve the six discrete components of drosophila aversive memory. Cell Rep *11*, 1280–1292.

65. Berry, J.A., Phan, A., and Davis, R.L. (2018). Dopamine neurons mediate learning and forgetting through bidirectional modulation of a memory trace. Cell Rep *25*, 651–662.e5.

66. Handler, A., Graham, T.G.W., Cohn, R., Morantte, I., Siliciano, A.F., Zeng, J., Li, Y., and Ruta, V. (2019). Distinct dopamine receptor pathways underlie the temporal sensitivity of associative learning. Cell *178*, 60–75.e19.

67. Cervantes-Sandoval, I., Davis, R.L., and Berry, J.A. (2020). Rac1 impairs forgetting-induced cellular plasticity in mushroom body output neurons. Front. Cell. Neurosci. *14*, 258.

68. Owald, D., and Waddell, S. (2015). Olfactory learning skews mushroom body output pathways to steer behavioral choice in *Drosophila*. Curr. Opin. Neurobiol. *35*, 178–184.

69. Tully, T., and Quinn, W.G. (1985). Classical conditioning and retention in normal and mutant *Drosophila melanogaster*. J. Comp. Physiol. A *157*, 263–277.

70. Scheunemann, L., Skroblin, P., Hundsrucker, C., Klussmann, E., Efetova, M., and Schwärzel, M. (2013). AKAPS act in a two-step mechanism of memory acquisition. J. Neurosci. *33*, 17422–17428.

71. Das, G., Klappenbach, M., Vrontou, E., Perisse, E., Clark, C.M.M., Burke, C.J., and Waddell, S. (2014). *Drosophila* Learn opposing components of a compound food stimulus. Curr. Biol. *24*, 1723–1730.

72. Galili, D.S., Dylla, K.V., Lüdke, A., Friedrich, A.B., Yamagata, N., Wong, J.Y.H., Ho, C.H., Szyszka, P., and Tanimoto, H. (2014). Converging circuits mediate temperature and shock aversive olfactory conditioning in *Drosophila*. Curr. Biol. *24*, 1712–1722.

73. Zhao, C., Widmer, Y.F., Diegelmann, S., Petrovici, M.A., Sprecher, S.G., and Senn, W. (2021). Predictive olfactory learning in *Drosophila*. Sci. Rep. *11*, 6795.

74. Mao, Z., and Davis, R.L. (2009). Eight different types of dopaminergic neurons innervate the *Drosophila* mushroom body neuropil: anatomical and physiological heterogeneity. Front. Neural Circuits *3*, 5.

75. Dylla, K.V., Raiser, G., Galizia, C.G., and Szyszka, P. (2017). Trace conditioning in drosophila induces associative plasticity in mushroom body kenyon cells and dopaminergic neurons. Front. Neural Circuits *11*, 42.

76. Chen, T.W., Wardill, T.J., Sun, Y., Pulver, S.R., Renninger, S.L., Baohan, A., Schreiter, E.R., Kerr, R.A., Orger, M.B., Jayaraman, V., et al. (2013). Ultrasensitive fluorescent proteins for imaging neuronal activity. Nature *499*, 295–300.

77. Kitamoto, T. (2001). Conditional modification of behavior in drosophila by targeted expression of a temperature-sensitive shibire allele in defined neurons. J. Neurobiol. *47*, 81–92.

78. Otto, N., Pleijzier, M.W., Morgan, I.C., Edmondson-Stait, A.J., Heinz, K.J., Stark, I., Dempsey, G., Ito, M., Kapoor, I., Hsu, J., et al. (2020). Input connectivity reveals additional heterogeneity of dopaminergic reinforcement in *drosophila*. Curr. Biol. *30*, 3200–3211.e8.

79. Vogt, K., Schnaitmann, C., Dylla, K.V., Knapek, S., Aso, Y., Rubin, G.M., and Tanimoto, H. (2014). Shared mushroom body circuits underlie visual and olfactory memories in Drosophila. eLife *3*, 3–5.

80. Mohammad, F., Stewart, J.C., Ott, S., Chlebikova, K., Chua, J.Y., Koh, T.W., Ho, J., and Claridge-Chang, A. (2017). Optogenetic inhibition of behavior with anion channelrhodopsins. Nat. Methods *14*, 271–274.

81. Klapoetke, N.C., Murata, Y., Kim, S.S., Pulver, S.R., Birdsey-Benson, A., Cho, Y.K., Morimoto, T.K., Chuong, A.S., Carpenter, E.J., Tian, Z., et al. (2014). Independent optical excitation of distinct neural populations. Nat. Methods *11*, 338–346.

82. Weiglein, A., Thoener, J., Feldbruegge, I., Warzog, L., Mancini, N., Schleyer, M., and Gerber, B. (2021). Aversive teaching signals from individual dopamine neurons in larval *Drosophila* show qualitative differences in their temporal "fingerprint". J. Comp. Neurol. *529*, 1553–1570.

83. Schroll, C., Riemensperger, T., Bucher, D., Ehmer, J., Völler, T., Erbguth, K., Gerber, B., Hendel, T., Nagel, G., Buchner, E., and Fiala, A. (2006). Light-induced activation of distinct modulatory neurons triggers appetitive or aversive learning in *drosophila* larvae. Curr. Biol. *16*, 1741–1747.

84. Hruschka, D.J., Branford, S., Smith, E.D., Wilkins, J., Meade, A., Pagel, M., and Bhattacharya, T. (2015). Detecting regular sound changes in linguistics as events of concerted evolution. Curr. Biol. *25*, 1–9.

85. Ueoka, Y., Hiroi, M., Abe, T., and Tabata, T. (2017). Suppression of a single pair of mushroom body output neurons in *Drosophila* triggers aversive associations. FEBS Open Bio *7*, 562–576.

86. Awata, H., Takakura, M., Kimura, Y., Iwata, I., Masuda, T., and Hirano, Y. (2019). The neural circuit linking mushroom body parallel circuits induces memory consolidation in Drosophila. Proc. Natl. Acad. Sci. USA *116*, 16080–16085.

87. Konorski, J. (1967). Integrative Activity of the Brain: an Interdisciplinary Approach (University of Chicago Press).

88. Dickinson, A., and Dearing, M.F. (1979). Appetitive-Aversive Interactions and Inhibitory Processes. Mechanisms of Learning and Motivation (Erlbaum), pp. 203–231.

89. Nasser, H.M., and McNally, G.P. (2012). Appetitive-aversive interactions in Pavlovian fear conditioning. Behav. Neurosci. *126*, 404–422.

90. Zhang, X., Kim, J., and Tonegawa, S. (2020). Amygdala reward neurons form and store fear extinction memory. Neuron *105*, 1077–1093.e7.

91. Gerber, B., Yarali, A., Diegelmann, S., Wotjak, C.T., Pauli, P., and Fendt, M. (2014). Pain-relief learning in flies, rats, and man: basic research and applied perspectives. Learn. Mem. *21*, 232–252.

92. Mayer, D., Kahl, E., Uzuneser, T.C., and Fendt, M. (2018). Role of the mesolimbic dopamine system in relief learning. Neuropsychopharmacology *43*, 1651–1659.

93. Dinsmoor, J.A. (2001). Stimuli inevitably generated by behavior that avoids electric shock are inherently reinforcing. J. Exp. Anal. Behav. *75*, 311–333.

94. Winston, J.S., Vlaev, I., Seymour, B., Chater, N., and Dolan, R.J. (2014). Relative valuation of pain in human orbitofrontal cortex. J. Neurosci. *34*, 14526–14535.

95. Riemensperger, T., Völler, T., Stock, P., Buchner, E., and Fiala, A. (2005). Punishment prediction by dopaminergic neurons in *drosophila*. Curr. Biol. *15*, 1953–1960.

96. Felsenberg, J., Barnstedt, O., Cognigni, P., Lin, S., and Waddell, S. (2017). Re-evaluation of learned information in *Drosophila*. Nature *544*, 240–244.

97. Bennett, J.E.M., Philippides, A., and Nowotny, T. (2021). Learning with reinforcement prediction errors in a model of the *Drosophila* mushroom body. Nat. Commun. *12*, 2569.

98. Krashes, M.J., DasGupta, S., Vreede, A., White, B., Armstrong, J.D., and Waddell, S. (2009). A neural circuit mechanism integrating motivational state with memory expression in *drosophila*. Cell *139*, 416–427.

99. Jenett, A., Rubin, G.M., Ngo, T.T.B., Shepherd, D., Murphy, C., Dionne, H., Pfeiffer, B.D., Cavallaro, A., Hall, D., Jeter, J., et al. (2012). A GAL4-driver line resource for *drosophila* neurobiology. Cell Rep *2*, 991–1001.

100. Pfeiffer, B.D., Truman, J.W., and Rubin, G.M. (2012). Using translational enhancers to increase transgene expression in *Drosophila*. Proc. Natl. Acad. Sci. USA *109*, 6626–6631.

101. Schindelin, J., Arganda-Carreras, I., Frise, E., Kaynig, V., Longair, M., Pietzsch, T., Preibisch, S., Rueden, C., Saalfeld, S., Schmid, B., et al. (2012). Fiji: an open-source platform for biological-image analysis. Nat. Methods *9*, 676–682.

102. Pfeiffer, B.D., Ngo, T.T., Hibbard, K.L., Murphy, C., Jenett, A., Truman, J.W., and Rubin, G.M. (2010). Refinement of tools for targeted gene expression in *drosophila*. Genetics *186*, 735–755.

103. Kang, L. (February 2008). The Image Stabilizer Plugin for ImageJ. http://www.cs.cmu.edu/~kangli/code/Image_Stabilizer.html.

104. Plaçais, P.Y., and Preat, T. (2013). To favor survival Under food shortage, the brain disables costly memory. Science *339*, 440–442.

Please cite this article in press as: Villar et al., Differential coding of absolute and relative aversive value in the *Drosophila* brain, Current Biology (2022), https://doi.org/10.1016/j.cub.2022.08.058

STAR★METHODS

KEY RESOURCES TABLE

REAGENT or RESOURCE	SOURCE	IDENTIFIER
Antibodies		
Mouse, α-Bruchpilot, nc82	Drosophila Studies Hybridoma Bank	Cat# nc82; RRID:AB_2314866
Chicken α-GFP	Abcam	Cat# ab13970; RRID:AB_300798
Normal Donkey Serum	Jackson immunoresearch	Cat# 017-000-121; RRID:AB_2337258
Alexa Fluor® 488 AffiniPure Donkey Anti-Chicken IgY (IgG) (H+L)	Jackson immunoresearch	Cat# 703-545-155; RRID:AB_2340375
Alexa Fluor® 647 AffiniPure Donkey Anti-Mouse IgG (H+L)	Jackson immunoresearch	Cat# 715-605-151; RRID:AB_2340863
Chemicals, peptides, and recombinant proteins		
Triton X-100	Sigma-Aldrich	Cat#T8787
PBS	Sigma-Aldrich	Cat#D8537
Paraformaldehyde 20% solution, EM grade	Electron microscopy	15713-S
VECTASHIELD Mounting Medium	Vector Laboratories	Cat# H-1000; RRID:AB_2336789
N-Tris	Sigma-Aldrich	Cat#T5691
NaCl	Sigma-Aldrich	Cat#S7653
KCl	Sigma-Aldrich	Cat#P9333
NaHCO3	Sigma-Aldrich	Cat#S6297
NaH2PO4	Sigma-Aldrich	Cat#S8282
CaCl2	Sigma-Aldrich	Cat#21115
MgCl2	Sigma-Aldrich	Cat#M1028
Trehalose	Sigma-Aldrich	Cat#T9531
Glucose	Sigma-Aldrich	Cat#G7528
TES	Sigma-Aldrich	Cat#T1375
Mineral Oil	Sigma-Aldrich	Cat#M5904
4-methylcyclohexanol (98%)	Sigma-Aldrich	Cat#218405
3-octanol (99%)	Sigma-Aldrich	Cat#153095
Isopentyl acetate (99%)	Sigma-Aldrich	Cat#306967
Agar	Fisher Scientific	Cat#10346693
Yeast	Dutscher	Cat#789196
Maize Flour	Limagrain ingredients	Cat#WFMZ01HS
Dextrose	Sigma-Aldrich	Cat#D9434
Tegosept	Dutscher	Cat#789063
All-trans-Retinal	molekula	Cat#116-31-4
Experimental models: organisms/strains		
D. melanogaster: Canton-S	Scott Waddell at University of Oxford,UK	N/A
D. melanogaster: c061-GAL4; MB-GAL80	Scott Waddell at University of Oxford,UK [98]	N/A
D. melanogaster: MB296B-GAL4	Bloomington Drosophila Stock Center[56]	RRID:BDSC_68308
D. melanogaster: MB058B-GAL4	Bloomington Drosophila Stock Center[56]	RRID:BDSC_68278
D. melanogaster: MB112C-GAL4	Scott Waddell at University of Oxford,UK[53]	N/A
D. melanogaster: MB077B-GAL4	Bloomington Drosophila Stock Center[56]	RRID:BDSC_68283
D. melanogaster: MB080C-GAL4	Bloomington Drosophila Stock Center[56]	RRID:BDSC_68285
D. melanogaster: MB018B-GAL4	Bloomington Drosophila Stock Center[56]	RRID:BDSC_68296
D. melanogaster: MB504B-GAL4	Bloomington Drosophila Stock Center[56]	RRID:BDSC_68329
D. melanogaster: R58E02-GAL4	Bloomington Drosophila Stock Center[42,99]	RRID:BDSC_41347
D. melanogaster: NP5272-GAL4	Kyoto DGGR[38]	RRID:DGGR_113659
D. melanogaster: MB630B-GAL4	Bloomington Drosophila Stock Center[41,56]	RRID:BDSC_68334

(*Continued on next page*)

Please cite this article in press as: Villar et al., Differential coding of absolute and relative aversive value in the *Drosophila* brain, Current Biology (2022), https://doi.org/10.1016/j.cub.2022.08.058

Continued

REAGENT or RESOURCE	SOURCE	IDENTIFIER
D. melanogaster: MB301B-GAL4	Bloomington Drosophila Stock Center[56]	RRID:BDSC_68311
D. melanogaster: 0104-GAL4	Insite collection (Scott Waddell at University of Oxford,UK)[43]	N/A
D. melanogaster: R56H09-GAL4	Bloomington Drosophila Stock Center[44,99]	RRID:BDSC_39166
D. melanogaster: 0279-GAL4	Insite collection (Scott Waddell at University of Oxford,UK)[21]	N/A
D. melanogaster: R56H09-GAL80	The present study	N/A
D. melanogaster: MB312B-GAL4	Bloomington Drosophila Stock Center[56]	RRID:BDSC_68314
D. melanogaster: MB056B-GAL4	Bloomington Drosophila Stock Center[56]	RRID:BDSC_68276
D. melanogaster: MB109B-GAL4	Bloomington Drosophila Stock Center[56]	RRID:BDSC_68261
D. melanogaster: 0804-GAL4	Insite collection (Scott Waddell at University of Oxford,UK)[44]	N/A
D. melanogaster: MB315C-GAL4	Bloomington Drosophila Stock Center[56]	RRID:BDSC_68316
D. melanogaster: MB087C-GAL4	Bloomington Drosophila Stock Center[56]	RRID:BDSC_68366
D. melanogaster: R66C08-GAL4	Bloomington Drosophila Stock Center[63,99]	RRID:BDSC_49412
D. melanogaster: pJFRC100-20XUAS-TTS-Shibire-ts1-p10 su(Hw)attP1	Gerald Rubin at Janelia Research Campus, Ashburn, Virginia, USA[100]	N/A
D. melanogaster: UAS-GCaMP6m	Bloomington Drosophila Stock Center[76]	RRID:BDSC_4970
D. melanogaster: UAS-GtACR1	Adam Claridge-Chiang at Duke-NUS Medical School, Singapore[80]	N/A
D. melanogaster: UAS-mCD8::GFP; 247-LexA, LexAop-rCD2::RFP	Scott Waddell at University of Oxford,UK[98]	N/A
D. melanogaster: UAS-csChrimson::tdTomato	Scott Waddell at University of Oxford,UK[53]	N/A
Software and algorithms		
GraphPad Prism 9.1.2.	GraphPad Software, La Jolla, CA	RRID:SCR_002798; https://www.graphpad.com/scientific-software/prism/
Fiji	Fiji (Image processing and analysis in Java) NIH; [101]	RRID:SCR_003070; https://fiji.sc
ZEISS ZEN Imaging Software	Carl Zeiss, Oberkochen, Germany	RRID:SCR_013672; https://www.zeiss.com/microscopy/int/products/microscope-software/zen.html
Arduino 1.8.9	Arduino.cc	RRID:SCR_017284; https://www.arduino.cc/en/Guide/ArduinoUno
MATLAB	Mathworks	RRID:SCR_001622; http://www.mathworks.com/products/matlab/
Inkscape	Inkscape	RRID:SCR_014479; https://inkscape.org/en/
Recombinant DNA		
pBPGAL80Uw-6	Gift from Gerald Rubin (Janelia Research Campus)	
Deposited data		
All behavioral and calcium imaging data and codes	https://github.com/	https://github.com/ManuPerisse/Absolute-and-relative-value-coding

RESOURCE AVAILABILITY

Lead contact

Further information and requests for resources and reagents should be directed to, and will be fulfilled by, the lead contact, Emmanuel Perisse (emmanuel.perisse@igf.cnrs.fr).

Materials availability

All original reagents presented in this study are available from the lead contact upon request.

Please cite this article in press as: Villar et al., Differential coding of absolute and relative aversive value in the *Drosophila* brain, Current Biology (2022), https://doi.org/10.1016/j.cub.2022.08.058

Data and code availability

- Behavioral and calcium imaging data reported in this paper have been deposited on GitHub and are publicly available as of the date of publication. The access link is listed in the key resources table.
- Detailed codes are available at https://github.com/ManuPerisse/Absolute-and-relative-value-coding.
- Any additional information required to reanalyze the data reported in this work paper is available from the lead contact upon request.

EXPERIMENTAL MODEL AND SUBJECT DETAILS

Animals

Fly stocks were cultured at 21°C on standard cornmeal food which was made with 40L of tap water, 280g of agar, 1.5kg of yeast, 2kg of corn flour, 2.8kg of Dextrose, 120g of Tegosept and 460mL of Ethanol. Genotypes and sources of the fly lines used in this study are denoted in the key resources table.

METHOD DETAILS

Fly construct

The R56H09-GAL80 construct was made by amplifying the R56H09 enhancer region from the genomic DNA of R56H09-Gal4 flies[102] using forward primer 5'-CACCGGCTACCACACCCAGCGTGCAACAG-3' and reverse primer 5'-CCTCCTTGATCAGGCGCGAAC AGGT-3'. The PCR product was cloned into pENTR/D-TOPO vector (pENTR™ Directional TOPO® Cloning Kits, Invitrogen). Then the enhancer fragment was put into pBPGal80Uw-6 plasmid (Addgene) using Gateway cloning system (Gateway™ LR Clonase™ II Enzyme Mix, Invitrogen). The R56H09-GAL80 plasmid was inserted into the attp40 landing site by site-specific integration (Bestgene).

Behavioral Analyses

Behavioral experiments were performed as previously described[21] with minor modifications. For all experiments, groups of ~100 5–10 day old flies were housed for 18–24 h before training in a 25 ml vial containing standard cornmeal food and a 20 x 60 mm piece of filter paper at 23°C and 65% relative humidity and a 12 h/12 h light-dark cycle (except for optogenetic experiments for which flies were raised in the dark prior to the experiment).

For the csChrimson experiments, 2-3 days old flies were placed in the dark on a 1mM all trans-Retinal solution (molekula, UK) mixed with fly food for 2 days prior to experiments. Electric shocks were delivered with a Grass S48 Square Pulse Stimulator (Grass Technology). For experiments in Figures 1A and 1B and all experiments using the thermogenetic tool Shi^{ts1}, we used a training tube with copper wires covering the inside of the tube. For the experiments in Figures 1A and 1B, flies were trained at 23°C and 65% relative humidity as follows: 1 min odor X with 12 x 1.5 s shocks (at 0.2 Hz) of either 15V, 30V, 60V or 90V, followed by 45 s air, and 1 min odor Y without reinforcement.

For the Shi^{ts1} experiments at restrictive temperature, flies were transferred 30 min prior to and during training into a behavioral room at 33°C and 65% relative humidity. Flies were trained as follows: 1 min odor X unpaired, followed by 45 s air, 1 min of odor Y with 12 x 1.5 s 60V shocks (at 0.2 Hz), followed by 45 s air, and 1 min odor Z with 12 x 1.5 s 30V shocks (at 0.2 Hz).

For the optogenetic experiments, we designed a transparent shock grid made of a 75 mm x 50 mm polyethylene terephthalate (PET) coated with a conductive indium tin oxide (ITO) 175μm film of 80 Ohms / Sq (Diamond Coatings Ltd., UK). A grid was laser-etched onto the ITO film in order to insulate the positive and negative electrodes (lanes in the grid were 0.5 mm spaced by 0.3 mm apart). Flies were trained at 23°C and 65% relative humidity as follows: 1 min odor X unpaired, followed by 45 s air, 1 min of odor Y with 12 x 1.5 s 120V shocks (at 0.2 Hz), followed by 45 s air, and 1 min odor Z with 12 x 1.5 s 60V shocks (at 0.2 Hz). The GtACR1 optogenetic stimulation was provided by 4 green LEDs at 101.85μW/mm^2 (λ = 525nm; Prolight Opto, PM2B-3LxE-SD, Technology Corporation, Taiwan) constantly illuminating the entire training tube during the presentation of odor Y or Z. The csChrimson optogenetic stimulation was provided by 4 red LEDs at 229.18μW/mm^2 (λ = 623nm; Prolight Opto, PM2B-3LRE-SD, Technology Corporation, Taiwan) and delivered at 0.5 Hz, with 1 s duration over the entire training tube during the presentation of odor Z + 60V. For the experiment in Figure 6B, odor X was paired for 1 min with red LED stimulation delivered at 0.5 Hz, with 1 s duration. After 45 s of fresh air, odor Y was presented alone for 1 min. The odor preference test was performed immediately after training.

Memory performance (immediately or 30 min after conditioning) was tested in the dark by allowing the flies to choose for 2 min between two of the odors presented during training: X vs Y for Figures 1A and 1B, relative choice Y vs Z and absolute choices X vs Y or X vs Z for all other behavioral experiments. A Performance Index (PI) was calculated as the number of flies making the correct choice minus the number of flies making the wrong choice, divided by the total number of flies in each experiment. A single PI value is the average score from flies of the identical genotype tested with the reciprocal reinforced/non-reinforced odor combination.

Odors used for conditioning were 3-octanol (OCT; 8 μl in 10 ml mineral oil), 4-methylcyclohexanol (MCH; 9 μl in 8 ml mineral oil) and isoamyl acetate (IAA; 16 μl in 10 ml mineral oil). Only 3-octanol and 4-methylcyclohexanol were used during testing.

Please cite this article in press as: Villar et al., Differential coding of absolute and relative aversive value in the *Drosophila* brain, Current Biology (2022), https://doi.org/10.1016/j.cub.2022.08.058

Immunohistochemistry and confocal microscopy

4-6 day old female fly brains were dissected in ice-cold PBS and fixed in 4% paraformaldehyde solution in PBS at room temperature for 20 min. Fixed brains were then incubated in a blocking solution in 10% donkey serum (Jackson Immunoresearch) in PBS-triton (PBST) 0.5% for 30 min at room temperature. Brains were then incubated with primary antibodies, α-Bruchpilot, nc82, (1:30, mouse, DSHB) and α-GFP (1:1000, Chicken, ABCAM) in PBST for 72 h at 4°C. After 3 x 10 min washes in PBST, brains were incubated with secondary antibodies, Alexa Fluor 647-conjugated donkey α-mouse and Alexa Fluor 488-conjugated donkey α-chicken (both at 1:400; Jackson Immunoresearch) overnight at 4°C. After 3 x 10 min washes in PBS, brains were mounted in Vectashield (Vector Labs) on a glass slide. Fly brains were imaged with a Leica SP8-UV confocal microscope. Image resolution was 1024 x 512 with 0.5 μm step size and a frame average of 3 with a 40x objective. All images were analyzed using Fiji.[101]

In vivo two-photon calcium imaging

Functional-imaging experiments were performed as described previously[47,53] with some minor modifications. 1-day old flies were transferred into vials containing standard food (maximum of 30 flies per vial) and imaged 4-7 days later. Flies were briefly immobilized on ice (30-60 s) and mounted in a custom-made chamber allowing free antennae and leg movement. The head capsule was opened under room temperature buffer solution (5 mM TES, 103 mM NaCl, 3 mM KCl, 1.5 mM $CaCl_2$, 4 mM $MgCl_2$, 26 mM $NaHCO_3$, 1 mM NaH_2PO_4, 8 mM Trehalose, 10mM glucose, pH 7). Membranes and trachea above the recording areas were manually removed. Individual flies in the recording chamber were placed under the 20x objective of a two-photon microscope (Zeiss LSM 710mp) and an electric shock grid (in copper) was positioned in contact with the fly's legs (visualized with a camera AV MAKO U-029B (Stemmer Imaging)). For all flies, GCaMP6m fluorescence signal was measured in a randomly chosen brain hemisphere. Fluorescence was excited by a Ti-Sapphire laser (Chameleon Ultra II, Coherent) using ~140fs pulses, 80MHz repetition rate and centered at 920 nm. Images of 256 x 256 pixels were acquired at 6.34Hz controlled with Zen software (Zeiss). Odors were delivered to the fly on a clean air stream at 0.9mL/min using the 206A olfactometer (Aurora Scientific). Electric shocks were delivered with a DS2A isolated voltage stimulator controlled with a DG2A train/delay generator (both from Digitimer, Ltd). Imaging (Zen software), electric shocks and odor delivery were all controlled via TTL signals using an Arduino board (Arduino uno Rev3, Arduino.cc) combined with a project board (K&H-102) and Arduino custom-made codes.

For imaging electric shock responses in DANs, each fly was recorded for 30 s before the onset of a 1 min sequence of 12 x 1.5 s electric shocks of a given voltage at 0.2 Hz. Note that in Figure 1, each fly was only tested for their response to one voltage intensity.

For imaging odor-evoked responses in MBONs following a differential training protocol, flies were first trained under the microscope with the same protocol as in Figures 1A and 2B. Flies were exposed to odor X for 1 min paired with 12 x 1.5 s electric shocks at 0.2 Hz (CS+), followed by 45 s of clean air and a second odor Y unpaired (CS-) for 1 min. Recording during the test started 1 min after the conditioning protocol. Flies were then exposed twice to a 5 s presentation of the CS+ and CS- with 30 s clean air exposure in between every odor (see Figures 2B and S2). Note that each fly was trained and recorded only once with a randomly chosen intensity of electric shock voltage during conditioning.

For imaging odor-evoked responses in PAM-β′2aγ5n DANs (MB109B-GAL4), MBON-γ2α′1 (MB077B-GAL4), MBON-γ1ped>αβ (MB112C-GAL4) and MBON-γ5β′2a (R66C08-GAL4) during training, flies were subjected to the following protocol (same as for the behavioral experiments in Figures 3, 4, and 5): 1 min odor X unpaired (IAA) followed by 45 s of clean air, then 1 min presentation of second odor Y (MCH) paired with 12 x 1.5 s 60V electric shocks at 0.2 Hz, followed by 45 s of clean air and 1 min of a third odor Z (OCT) paired with 12 x 1.5 s 30V electric shocks at 0.2 Hz. To investigate the "worse than" neural mechanisms in Figure 6A, the odor Y was paired with 12 x 1.5 s 30V electric shocks at 0.2 Hz and the odor Z with 12 x 1.5 s 60V electric shocks at 0.2 Hz. Note that each fly was trained and recorded only once.

Recorded images were manually segmented with Fiji using a custom-made code including an image stabilizer plugin.[103] For each recording, one region of interest (ROI) was drawn around the zone expressing GCaMP6m (dendrites for MBON-γ1ped and MBON-γ2α′1 or axonal terminals for all DANs and for MBON-γ5β′2a) after image stabilization to generate the summed fluorescence at each frame. A second ROI of the same size was chosen in the background where no changes occur during the whole recording. The GCaMP6m fluorescence (F(t)) was then calculated by subtracting the background. Flies that did not respond to any odor presentations were excluded from the analysis. For subsequent analyses custom MATLAB (MathWorks, Inc) scripts were used to first calculate variation of calcium transient from the baseline F0 with the following equation: $\Delta F = (F(t) - F0) / F0$. In Figure 7, the MBON data correspond to a frame by frame subtraction of mean ΔF per animal for the mock and train groups for Z+30V – Y+60V, Y+60V – X+0V and Z+30V – X+0V.

For DANs recordings, the baseline fluorescence (F0) was defined as the mean fluorescence (F) from the 25 s before the start of the electric shock sequence. We chose this long duration for F0 as PPL1 DANs display rhythmic slow oscillatory activity[104] that could affect our ΔF calculation. For MBON recordings during training and testing, or PAM-β′2aγ5n DANs during training, F0 was defined as the mean fluorescence of the 2 s before each odor presentation. As we presented the CS+ and CS- twice in Figures 2 and S2 to record MBON odor-evoked responses after learning, we used MATLAB to average the odor responses of the two odor presentations. In all experiments we calculated the mean fluorescence and the area under the curve (integral F/F0) during the whole sequence of electric shocks or odor presentation (alone or combined with electric shocks during training).

Please cite this article in press as: Villar et al., Differential coding of absolute and relative aversive value in the *Drosophila* brain, Current Biology (2022), https://doi.org/10.1016/j.cub.2022.08.058

QUANTIFICATION AND STATISTICAL ANALYSIS

All statistical analyses were performed using PRISM 9.1.2 (GraphPad Software). All behavioral and imaging data were first tested for normality using the D'Agostino and Pearson normality test. Normally distributed data were analyzed with parametric one-way ANOVA followed by Tukey's honest significant difference (HSD) post hoc test. For non-Gaussian distributed data, Kruskal-Wallis test was performed followed by Dunn's multiple comparisons test. Simple linear regression was used to fit a model to our data (shock responses or CS+ CS- difference). We also compared linear regression slopes with Prism (equivalent method to an Analysis of covariance). For the correlation between calcium transient and shock intensities we used parametric Pearson or non-parametric Spearman correlation. Paired t- or Wilcoxon tests were used to compare MBON CS+ and CS- responses after training. Unpaired t- or Mann-Whitney tests were used to compare cell body counting and quarters of area under curve for fluorescence data during training. One sample t-test against 0 was used in Figures 6B–6D. All graphics were generated with Inkscape 1.0.2 (Inkscape). All statistical comparisons are presented in Table S1.